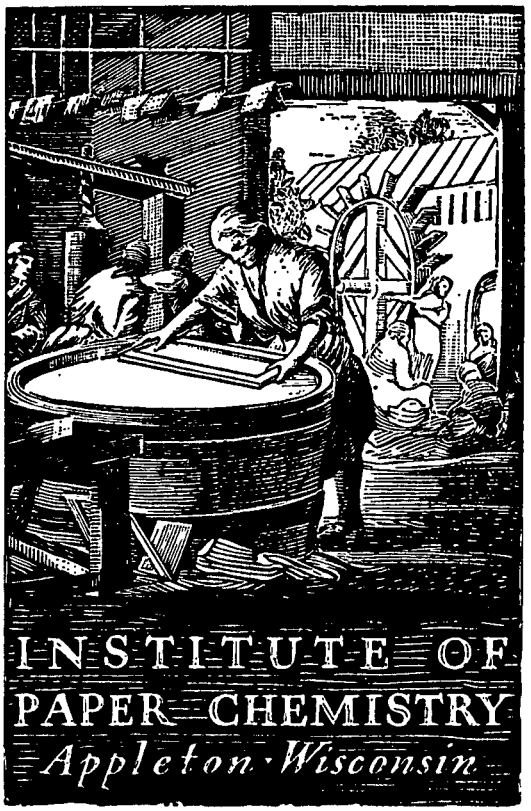

OUT-OF-PLANE SHEAR DEFORMATION BEHAVIOR OF PAPER AND BOARD

Project 3500

Report One
A Progress Report
to
MEMBERS OF THE INSTITUTE OF PAPER CHEMISTRY

May 1, 1983

THE INSTITUTE OF PAPER CHEMISTRY

Appleton, Wisconsin

OUT-OF-PLANE SHEAR DEFORMATION BEHAVIOR OF PAPER AND BOARD

Project 3500

Report One

A Progress Report

to

MEMBERS OF THE INSTITUTE OF PAPER CHEMISTRY

May 1, 1983

TABLE OF CONTENTS

LIST OF TABLES

LIST OF FIGURES

THE INSTITUTE OF PAPER CHEMISTRY

Appleton, Wisconsin

OUT-OF-PLANE SHEAR DEFORMATION BEHAVIOR OF PAPER AND BOARD

SUMMARY

The importance of out-of-plane shear deformation with respect to the characterization, converting, and end-use properties of paper and board, and the various methods which have been developed for its measurements, are reviewed. The torsion mode is suggested as one means of achieving pure shear deformation.

A method for determining the shear stress/strain behavior in the torsion mode has been developed. This utilizes our Instron 1125, together with a simple mechanical device employing capacitance type transducers to measure the small strains associated with shear deformation. Shear deformation measurements have been made on commercial linerboard, corrugating medium, and oriented handsheets made on the Formette Dynamique. In-plane and out-of-plane elastic properties were measured ultrasonically, and where appropriate, comparisons were made with properties determined mechanically. The effect of out-of-plane shear deformation on STFI compressive strength was also investigated.

The variation of the in-plane and out-of-plane elastic properties in the thickness direction was measured on commercial linerboard and corrugating medium samples where material had been symmetrically removed by surface grinding. Both in-plane longitudinal and shear moduli measured ultrasonically decreased with decreasing basis weight, i.e., toward the mid-plane of the sheet. It is hypothesized that this effect might be attributed to a variation in drying stress in the thickness direction of paper. The out-of-plane elastic moduli show a similar trend, i.e., they decrease with decreasing basis weight. In contrast, the shear modulus determined mechanically shows an opposite trend. The shear modulus of the linerboard is

essentially constant with decreasing basis weight, whereas the corrugating medium sample shows a significant increase. The apparent density of the linerboard sample is essentially constant, but that of the medium increases with decreasing basis weight. Ultrasonic and mechanical shear modulus measurements were made on oriented handsheets, where two drying restraint conditions were investigated (i.e., full restraint and zero restraint). The unrestrained handsheets had a slightly higher density and shear modulus (mechanical) than the sheets dried under restraint. Again, the opposite effect was found for the out-of-plane ultrasonic measurements; i.e., the restrained sheets gave higher values. The reason for the differences between the ultrasonic and mechanical measurements has not yet been determined. The effect of shear straining up to failure on the compressive strength level of corrugating medium was also investigated. No significant reduction in compressive strength was found, even though there was a reduction in specific shear modulus as measured ultrasonically.

During the course of the investigation it was also found that surface reinforcement of the samples by the mounting tissue adhesive significantly increased their compressive strength.

A limited light microscope and SEM study has also been conducted in an attempt to determine the mode of failure in shear.

INTRODUCTION

This report details our progress toward measuring the out-of-plane deformation behavior of paper and board. This deformation mode has until recently (1-8,14-16) received little attention. We are interested in the elastic, viscoelastic, and failure properties and their practical importance in converting and end-use properties. For example, in the fluting of corrugating medium it has been argued (9) that shear deformation may play an important role in this process as well as affecting the properties of the converted medium, particularly its compressive strength. During the fluting process the medium is also subjected to compressive, tensile, and bending stresses. Therefore, we should also be concerned with the contribution of shear to other combined stress situations. This investigation is also intended to complement ongoing work directed toward the characterization of paper and board using ultrasonic techniques. In this study we have used these latter methods to aid in characterizing our samples and for comparison, where possible, with the mechanically derived measurements.

BACKGROUND AND LITERATURE REVIEW

Out-of-Plane Shear Deformation Behavior of Paper and Board

A material subjected to a pure shear deformation is shown in Fig. 1.

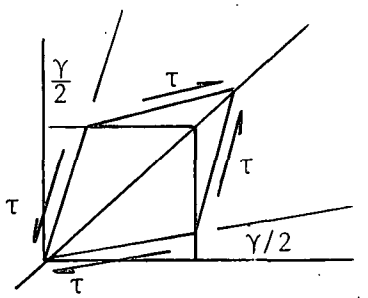

Figure 1. Pure shear deformation.

A shear modulus G may be defined for small strains as:

$$G = \frac{\tau}{\gamma} \tag{1}$$

where τ is the shear stress and γ is the shear strain.

In practice, a state of pure shear is difficult to achieve and usually other stresses are also present. The simple shear mode shown in Fig. 2 has been used by a number of researchers.

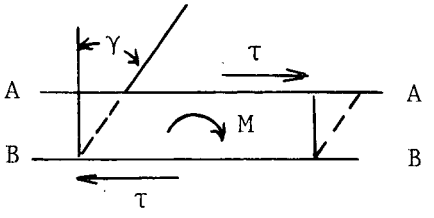

Figure 2. Simple shear mode.

In simple shear, a resultant moment M is present which has to be balanced. The shear modulus G is again defined by Eq. (1).

If the surfaces A-A and B-B move parallel to each other, then the bulk of the material will be subjected to a pure shear field and only the end regions (of the order of the thickness of the material) will be in a more complex stress state (10). However, if one is interested in failure properties, these end regions are also sources of stress concentration.

The following configuration is the one adopted by Byrd (Fig. 3) (1,6):

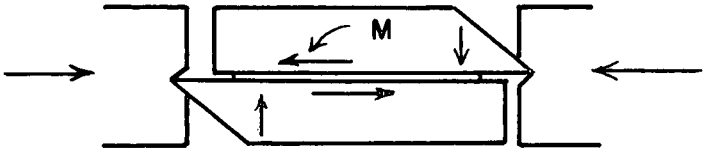

Figure 3. Byrd's configuration.

A state of shear is achieved by subjecting the sample holder to uniaxial compression. In this case the resultant moment M is balanced by a side thrust

imparted by the grooved blocks, which also subjects the sample to a (nonuniform) lateral compression. Fellers (2) used the simple shear mode and also developed an apparatus for loading specimens in tension using an Instron tensile tester.

The double lap shear configuration (3,5) has also been used in making shear measurements and appears to be attractive inasmuch as there will be no resultant moment, provided the materials to be evaluated are identical. There will, however, be nonuniform stresses in the end regions of the sample, as discussed for the single lap case.

The works of Byrd et al. (1,6) and Fellers (2) in developing a suitable method for shear deformation measurements have considered the problems of adhesion, surface preparation, and basis weight. They both use the heat-activated photographic mounting tissue method developed by Byrd (1). Their findings are basically in agreement. They recommend that surface grinding is necessary to improve adhesive contact and reduce variability. Both Byrd (1) and Fellers (2) find a dramatic rise in shear modulus and shear strength below a caliper of about 0.1 mm (~50 g/m^2), for both single and laminated sheets as shown in Fig. 4.

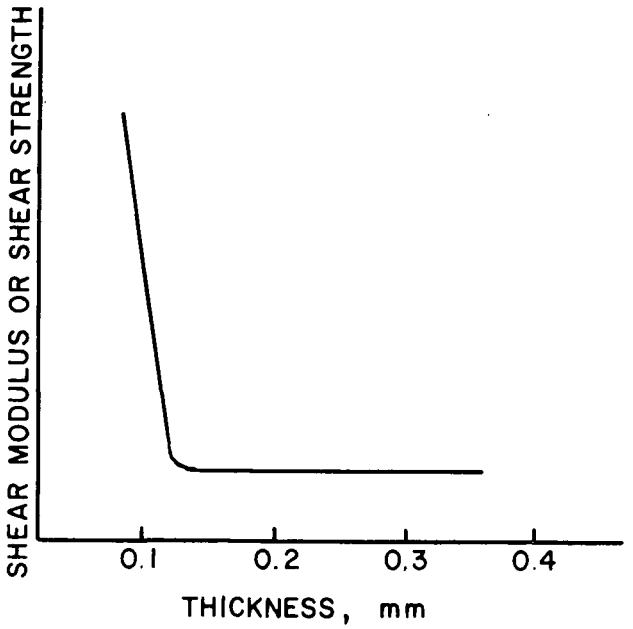

Figure 4. Effect of mechanical shear measurements.

Byrd argues that this can be attributed to the anchoring of fibers between the two adhesive layers. Fellers believes it may be due to a dramatic change in z-direction stress distributions (he also makes the analogy between this effect, and zero span and normal span tensile testing). No correction for the adhesive layer is mentioned in Fellers', work.

Byrd (6) has also examined the effects of fiber orientation and drying restraint on the shear deformation behavior of handsheets. These were made on the Formette Dynamique using a 47% unbleached Swedish pine kraft pulp which was beaten in a P.F.I. mill for 6000 revs. The basis weight was nominally 100 g/m^2. Orientation ratios of 1:1, 3:1, and 6:1 as defined by tensile ratios were produced. Byrd's results also show how apparent density varies with drying restraint and wet straining, a factor he did not discuss. His results show that for each level of fiber orientation there is a decrease in density as one goes from a freely dried condition to one of full restraint. The effects of wet straining are less clear-cut, and in some instances there is an increase in density with wet straining, the increase being most pronounced at the highest level of fiber orientation. It should be noted that these sheets were only held under restraint in the machine direction after wet straining. The work of Setterholm and Chilson (11) and Setterholm and Kuenzi (12) using TAPPI standard caliper measurements indicated the opposite effect; i.e., freely dried sheets had a lower density than restrained sheets. However, it should be noted that Byrd (6) was using a caliper measurement technique developed by Setterholm (13). We will discuss this point further in the results section, but on reflection it seems reasonable that the bonding level of freely dried sheets would be equal to, if not greater than, those dried under restraint. Bonding is basically established before shrinkage occurs. Fleischman's data (16) clearly show a monotonic

decrease in apparent density* with wet straining; however, his sheets were restrained in both directions after wet straining.

Byrd (6) reported that shear modulus and shear strength both decrease with increasing levels of wet straining, whereas tensile strength in the direction of straining increases. Shear modulus and shear strength increased with increasing fiber orientation. These findings are essentially in agreement with those of Fleischman (16), who used ultrasonic techniques to measure shear moduli. Mann, Baum, and Habeger (14) were the first to determine the out-of-plane shear moduli using ultrasonic techniques.

Perkins and McEvoy (4) and Uesaka (7) have used a torsional pendulum technique to measure both the in-plane and out-of-plane shear moduli for unbeaten spruce kraft handsheets having a basis weight of 228 g/m^2. The apparent density was varied by using different levels of wet pressing. The out-of-plane shear modulus varied linearly with apparent density in the range of 368 to 983 kg/m^3. This technique, of course, cannot be used to determine failure properties.

Failure properties alone have been measured by Heckers and Gottsching (3) using a double lap technique and by Wyk and Gerischer (8) using a simplifed form of Byrd's technique. In the former case the investigation was concerned with sample preparation variables, i.e., adhesive, pressure, and time. The latter paper was mainly concerned with the effects of recycling on paper properties, and it was found that the shear strength of paper decreased with increasing number of cycles.

Table I summarizes the various measurements of out-of-plane shear modulus made on paper and board. Where data for anisotropic sheets are included, a mean shear modulus has been calculated using Eq. (3) given in the following section.

*Based on IPC caliper measurements (22).

TABLE I

SUMMARY OF OUT-OF-PLANE SHEAR MODULUS MEASUREMENTS
MADE ON PAPER AND BOARD

Reference	Furnish	Density Kg/m^3	Mean Shear Modulus[a] GPa	Remarks
Byrd et al. (1)	Unbleached southern pine kraft	--	0.383	Ground surface pressed dried
Byrd et al. (1)	Unbleached kraft linerboard	--	0.138	M.D.?
Fellers (2)	Western hemlock	600	0.070	Handsheets
Perkins (4)	Spruce kraft pulp	368-983	0.0883-0.157	Indirect method using torsional pendulum, handsheets
Byrd (6)	Unbleached Swedish pine kraft	600-744	0.075-0.256	Orientated handsheets using Formette
Mann et al. (14)	Milk carton stock	780	0.115	Ultrasonic measurements
Mann (15)	Linerboard	625-691	0.0847-0.115	Ultrasonic measurements
Fleischman (16)	Bleached kraft Douglas-fir	430-950	0.095-0.425	Ultrasonic measurements, oriented handsheets using Formette

[a]Calculated using Eq. (3).

Torsion Deformation Mode

A number of methods developed for measuring the out-of-plane shear deformation behavior of paper and board were reviewed in the previous section, together with their shortcomings and results. Another possible method which does not appear to have been used for paper is the torsion mode. It can be shown that for certain cylindrical isotropic and orthotropic bodies a state of pure shear exists when they are subjected to torsion.

For the disk shown in Fig. 5 the out-of-plane shear modulus is calculated as follows:

$$G = \frac{T}{\theta}\frac{t}{J} \tag{2}$$

where T is the torque, θ the associated angular displacement, t the disk thickness, and J the polar second moment of area.

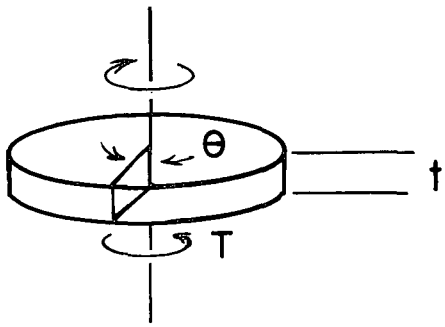

Figure 5. Torsion of thin disk.

For the case of an orthotropic disk in torsion, the measured or effective shear modulus is given according to Lekhnitskii (17) by the following equation:

$$\overline{G} = \frac{2G_{xz}G_{yz}}{G_{xz} + G_{yz}} \tag{3}$$

where G_{xz} and G_{yz} are the out-of-plane shear moduli in the machine and cross directions, respectively. If the anisotropy in the out-of-plane moduli is not too large,

then we see from Eq. (3) that the measured shear modulus will be a good approximation of the geometric mean of the out-of-plane moduli.

If we are interested in determining the components G_{xz} and G_{yz} on, say, machine-made paper or oriented handsheets using Eq. (3), we must also have a measure of G_{xz}/G_{yz}. We therefore look for a relationship between G_{xz}/G_{yz} and T_x/T_y, the in-plane tensile strength ratio which is commonly used incorrectly as a measure of fiber orientation.

Turning again to Fleischman's (16) results, the variation of G_{xz}/G_{yz} with T_x/T_y is shown in Fig. 6. For clarity, only the mean values have been plotted for Fleischman's ultrasonically determined G_{xz}/G_{yz} and Instron tensile ratios. Fleischman stated that the out-of-plane shear modulus ratio might be a good measure of fiber orientation because it is less sensitive to wet straining than T_x/T_y. In any case it seems possible to develop a reasonable correlation between G_{xz}/G_{yz} and T_x/T_y in order to calculate the components G_{yz} and G_{yz} as described above.

Details of our experimental technique for measuring the out-of-plane shear deformation behavior of paper, employing the torsion mode, are given in the next section.

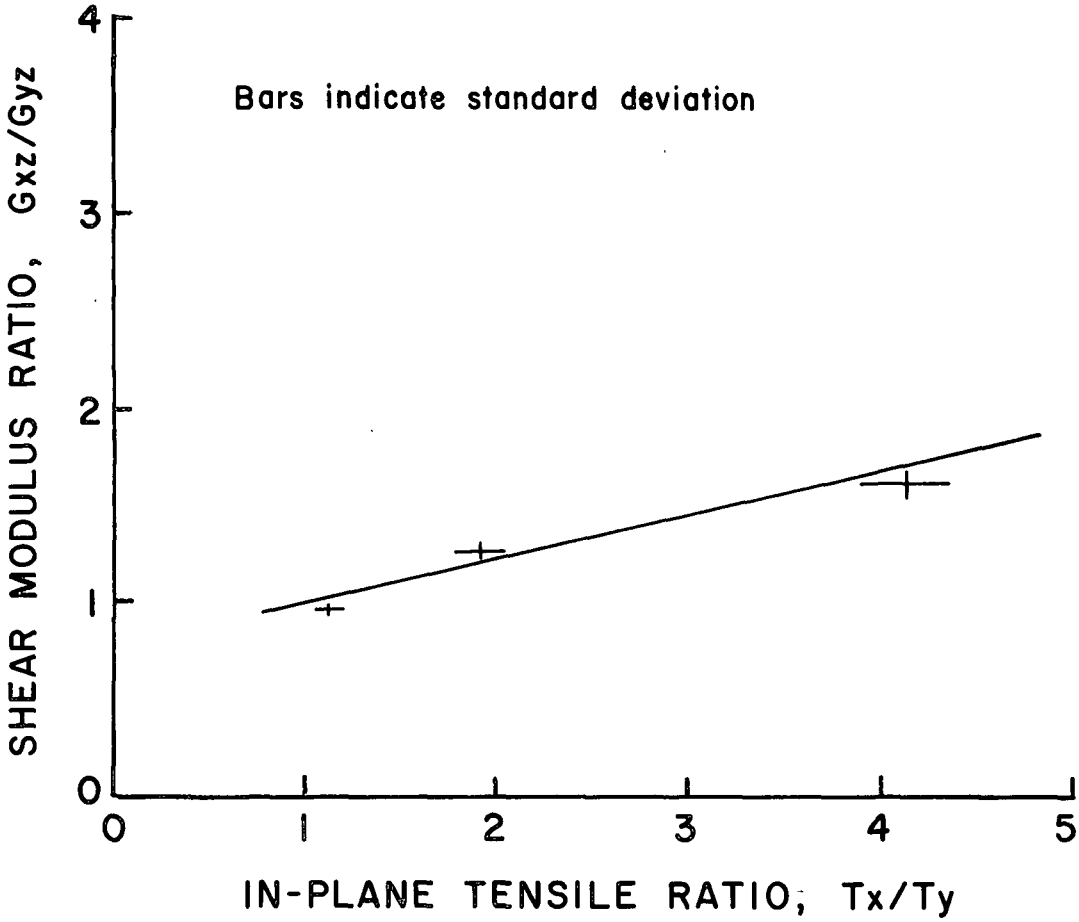

Figure 6. Out-of-plane shear modulus ratio variation with in-plane tensile ratio.

EXPERIMENTAL

The torsion method has been selected, following the discussion in the previous section, as a means of inducing a state of pure shear in the sample.

The general requirements for the measurement of the out-of-plane shear deformation behavior of paper and board using this method are as follows:

1. A suitable means of applying a controlled rate of strain to the sample and measuring the induced strain
2. A method for measuring the angular displacement of the sample
3. A method for recording the torque-angular displacement behavior of the sample

The fulfillment of these requirements will now be discussed in more detail. The method of applying a controlled rate of strain to the sample was in part satisfied by our decision to utilize the recently acquired floor model Instron 1125 which has torsion loading facilities and a torsion load cell as shown in Fig. 7.

Two sample configurations were tried, namely a ring and a disk, both having an outer diameter of 1.489 inches, as shown in Fig. 8. The width of the ring was nominally 0.25 inch.

The samples are mounted (as described below) between two cylinders*, as shown in Fig. 9. Ideally, one would like to have a simple and rapid means of mounting the samples. The use of friction only between sample and cylinders was considered but eliminated, because of the need to apply high ZD compressive loads to the sample. Whether or not the sample could be held between a "serrated" type of

*Precision ground cylinders were already in existence from a previous project.

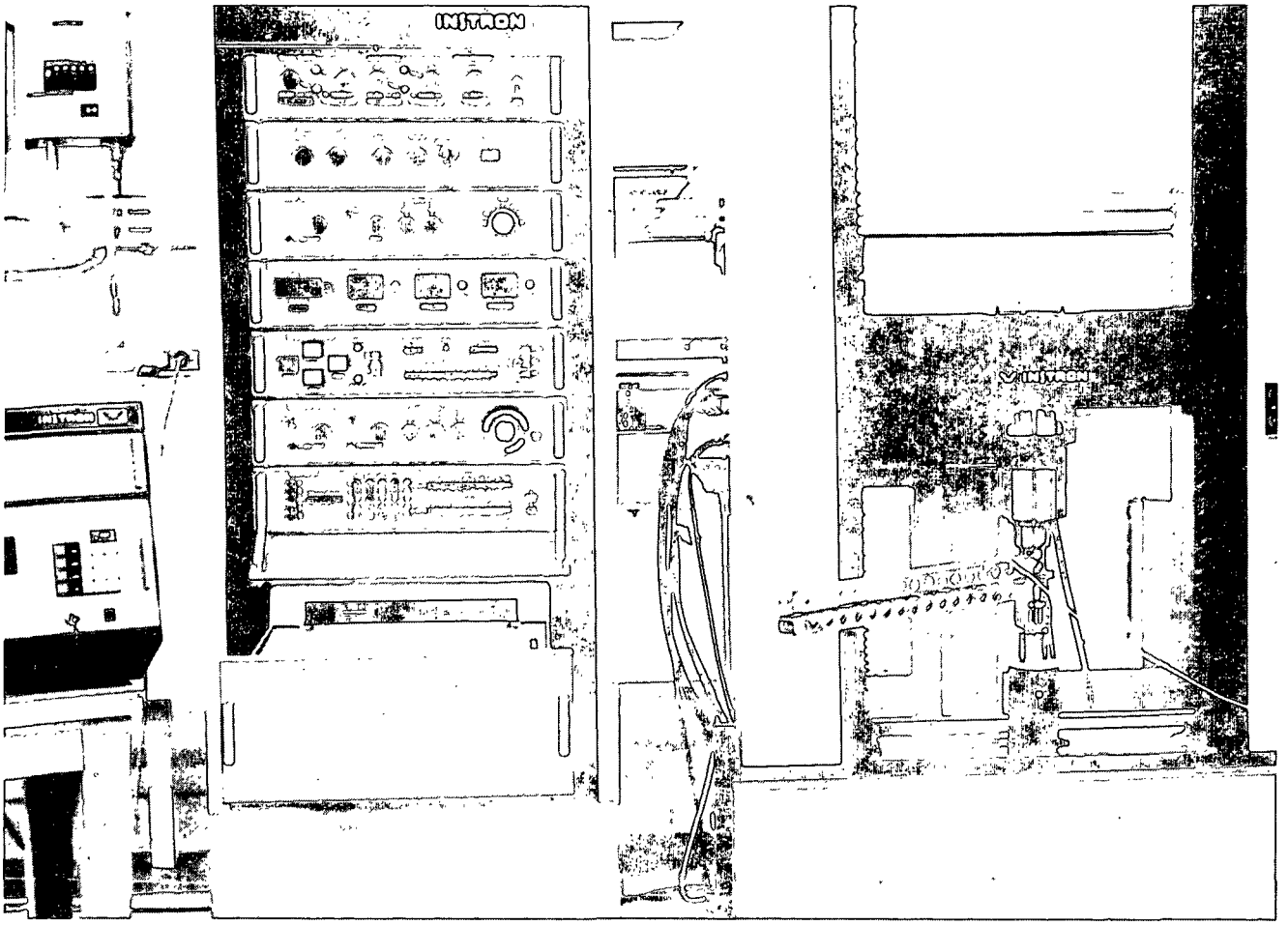

Figure 7. Floor model Instron 1125 with shear measuring device.

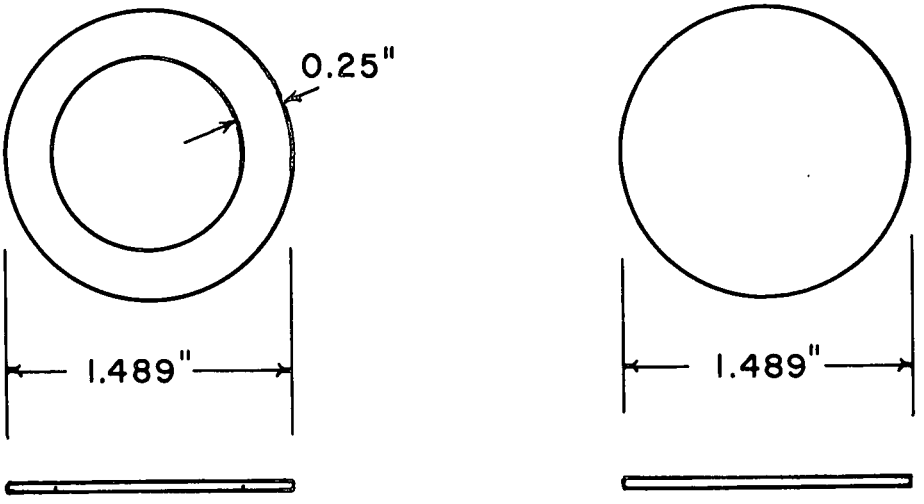

Figure 8. Sample configurations.

surface is a possibility which has not been explored. The mounting technique used is the photographic mounting tissue method developed by Byrd et al. (1). In our early experiments the Epoxy 907 adhesive system was used with some success, but the mounting tissue method is preferred because of the relative ease with which this adhesive can be removed from the sample after shear deformation testing. One major objection to the mounting tissue technique is that the samples are subjected to a heating and conditioning cycle before testing, with the possibility of degradation and/or crosslinking effects, although these effects are believed to be minimal here.

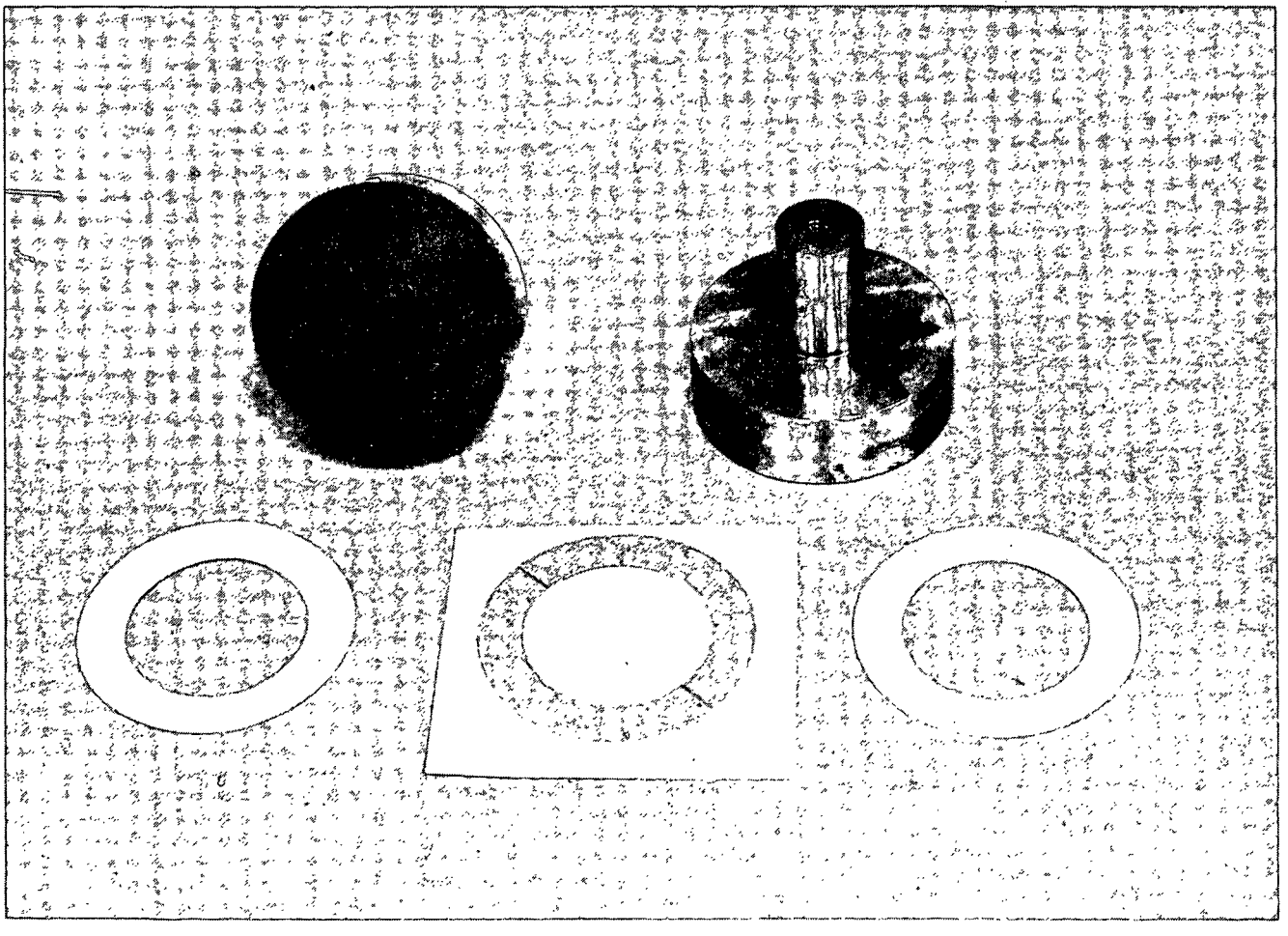

Figure 9. Mounting cylinders, ring samples and tissues.

Sample Mounting Procedure

The paper or board samples are either machined or cut to produce the ring or disk sample configurations shown in the above figure, together with two pieces of photographic mounting tissue. Two types of mounting tissue were investigated: the Seal MT-5 (Seal Inc., Shelton, Conn.) and Kodak photographic mounting tissue. However, in most of our testing we used the MT-5 because of its somewhat better adhesion to the steel mounting cylinders. The samples and mounting tissues are weighed and the caliper measured before mounting and heat activation. Two pairs of mounting cylinders, samples, and mounting tissues, are carefully aligned in a jig and dead loaded to a pressure of 17.5 psi, as shown in Fig. 10. This assembly is placed in an oven for 45 minutes at a temperature of 120°C to activate the mounting tissue adhesive.

After cooling, the mounted samples are allowed to equilibrate at TAPPI standard testing conditions for three days prior to testing. Sample plus tissue weights and calipers are measured to assess equilibrium conditions and the extent of adhesive penetration into the sample. The latter measurement requires that weights and calipers have also been obtained for the mounting tissues alone.

Instron 1125

Prior to testing in the Instron, the strain-measuring device described in the next section was carefully attached to the mounting cylinders, as shown in Fig. 11. It was important in assembling the mounted sample into the Instron that the sample would not be unintentionally loaded or torqued. This was difficult to achieve with the drill type chucks supplied with the Instron, which if used alone tended to torque the sample when they were tightened. This was eliminated by using a pin assembly in the lower chuck, as shown in Fig. 12. However, the shear strength

of the connecting screw was not sufficient* to allow a sample to be strained to failure, and so this method was only used to determine the initial shear modulus of the samples. When the samples were to be strained to, or near, failure, the mounted sample was tightened as carefully as possible into the lower drill chuck. Any residual torque could be removed by adjusting the Instron.

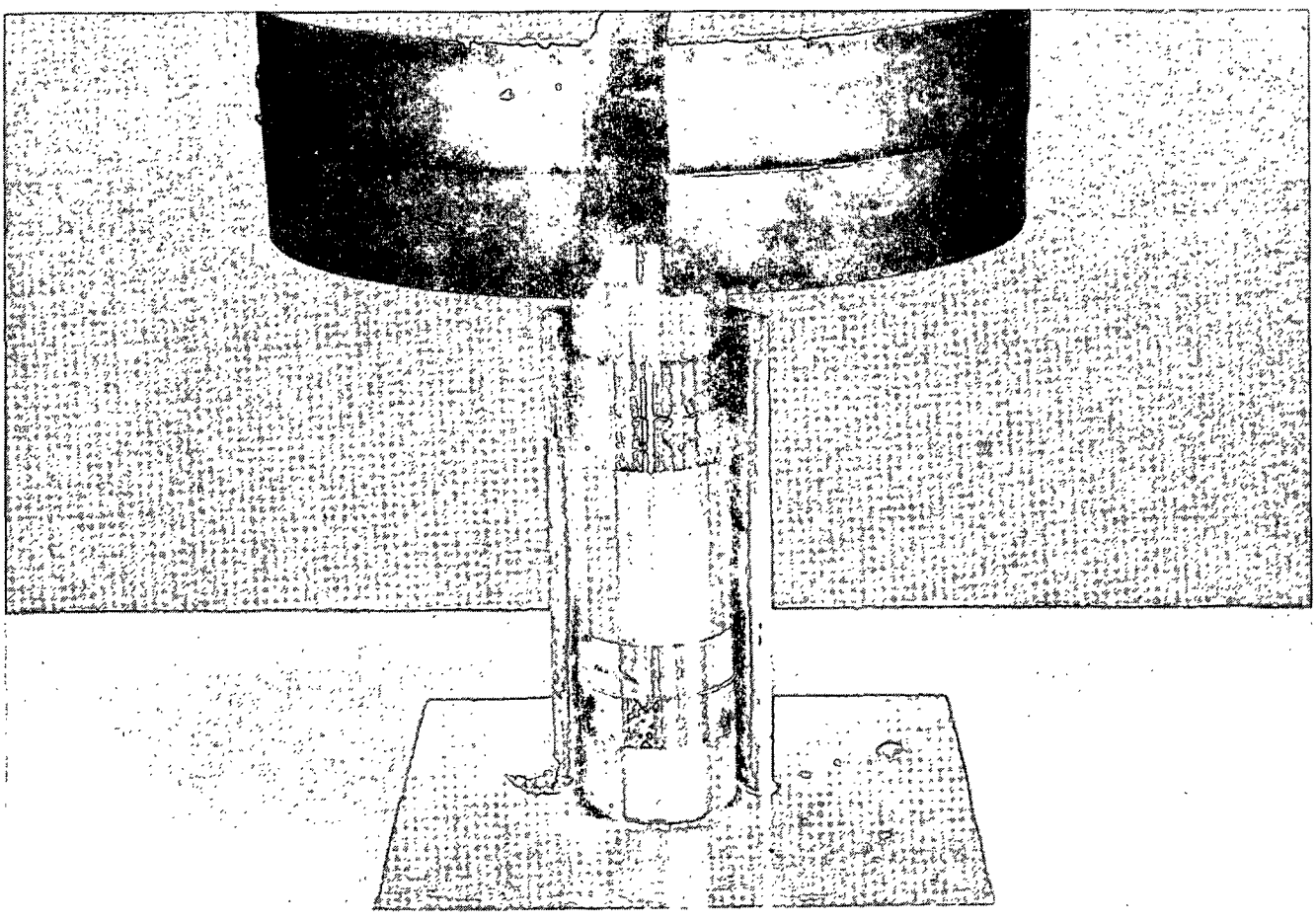

Figure 10. Mounting cylinders and jig for heat activation.

Before attempting to install the mounted sample into the Instron, it was important to check the alignment of the drill chucks. This requires shimming of the load cell to which the upper chuck is attached. The lower chuck is spring loaded and can be axially retracted to facilitate mounting. Adjustment of jaw spacing,

*This limitation was a consequence of using the already existing mounting cylinders.

together with the spring loading, insured that the sample was not axially loaded. After installing the mounted sample into the Instron, the locking screws and spacing blocks on the strain-measuring device were removed.

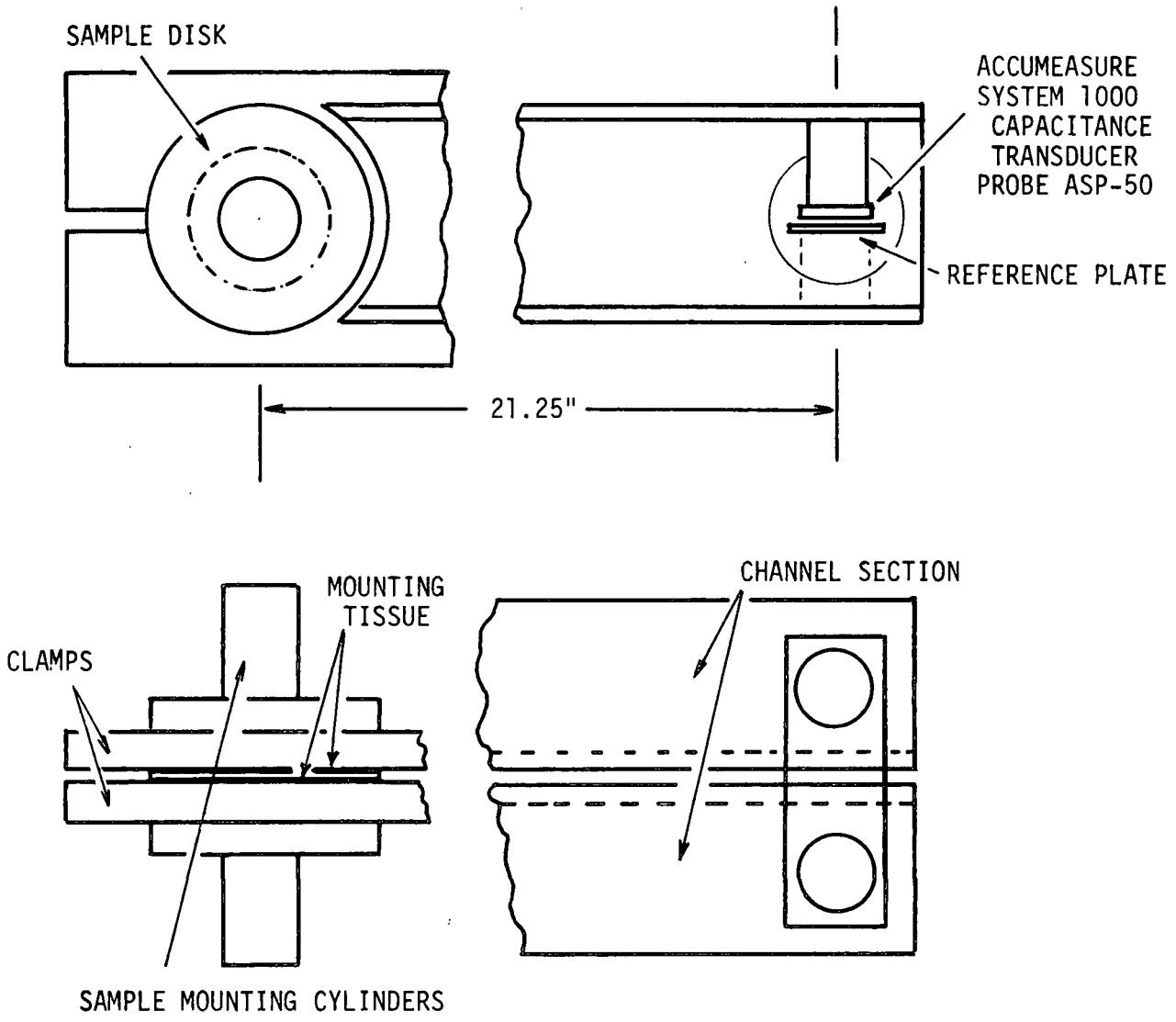

Figure 11. Schematic of strain-measuring device.

Shear strain measurements are more difficult than those for, say, tensile strain determination because of the very small deformations involved. For a disk sample of thickness t and radius r, subjected to a torque producing an angular

displacement $\Delta\theta$ radians the shear strain γ is given by:

$$\gamma = \frac{\Delta\theta r}{t}$$

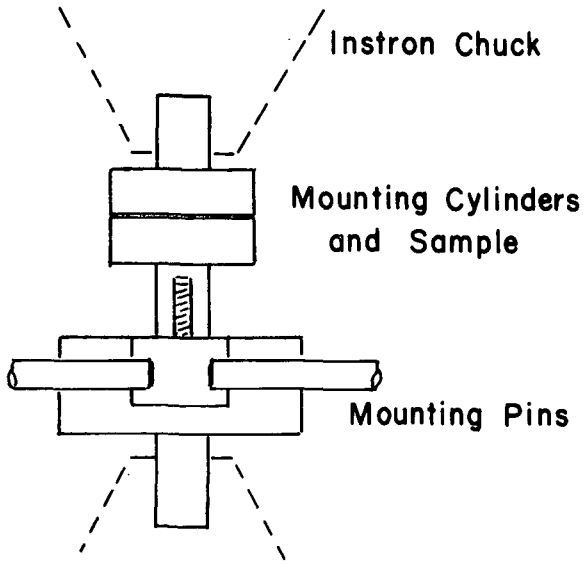

Figure 12. Pin mounting assembly.

For example, a 1.5-inch diameter disk having a thickness of 0.010 inch requires an angular displacement measurement of 10^{-6} radians to measure a strain level of 0.01%. The Instron, although it is capable of measuring angular displacement, would give the angular displacement of the chucks and assembly for torque transmission as well as the sample. We have therefore fabricated a simple mechanical device for amplifying and directly measuring the angular displacement of the sample (actually sample and mounting tissue). A schematic of the strain-measuring system is shown in Fig. 11.

It employs a capacitance type displacement transducer (Accumeasure probe ASP-50). This transducer has a maximum range of 0.050 inch with a 10-volt DC output and is used in conjunction with the Accumeasure 1000 system (Mechanical Technology Incorporated). The stated resolution is 50×10^{-6} inch.

The sensitivity of the strain-measuring device is calculated as follows. The angular displacement $\Delta\theta$ radians is given by

$$\Delta\theta = \frac{\Delta x}{R}$$

From the above $\Delta x = 5.0 \times 10^{-6}$ in./mV and R = 21.25 inch, so that

$$\Delta\theta = 0.235 \times 10^{-6} \text{ radians/mV}$$

In practice, the resolution is limited by the signal-to-noise ratio and was actually found to be close to the value stated by the manufacturer: 1×10^{-6} radians. Higher resolution probes are available.

Recording System

The rate of angular displacement was controlled through the Instron 1125, and the induced torque history was recorded directly by the Instron. The outputs from the torque load cell and the Accumeasure 1000 system were connected to a Hewlett Packard X - Y recorder to record the torque-angular displacement behavior of the sample. Exploratory dynamic measurements were also made, since the Instron was capable of strain cycling. In this case the above outputs were connected to a Brush Recorder.

Samples and Preparation

The investigation has been performed using commercial samples of linerboard and corrugating medium. In some instances these samples were surface ground (or machined) using techniques developed by Wink (18). Oriented handsheets were also made on the Formette Dynamique using an unbleached kraft pulp of 475 CSF. After wet pressing, the sheets were dried either with restraint (zero shrinkage) or without restraint.

Basis weight and caliper measurements were made on each sample. STFI compressive strength measurements were made on equipment manufactured by Lorentzen and Wettre.

DISCUSSION OF RESULTS

The method for making shear deformation measurements was given in the experimental section. As the work progressed, improvements were made in sample preparation and mounting procedures which improved the accuracy and reproducibility of the measurements. The method allows the torque-angular displacement behavior of the sample to rupture to be recorded (see Fig. 23). From this we can calculate the initial mean shear modulus, the maximum shear stress, and shear strain at failure. Strain cycling is also possible.

In connection with the influence of the corrugating operation on medium properties (9) we have also been interested in examining the effects of shear deformation on compressive strength. In addition to the above, the effects of sample configuration, sample preparation by surface grinding, and property changes in the thickness direction, and the influence of the mounting tissue on shear deformation behavior are discussed.

Sample Configuration

Two sample configurations have been investigated as described in the experimental section. The initial investigation was performed using the ring type sample. This was chosen with the idea of minimizing the variation of strain across the sample and for convenience in subsequent testing. Shear modulus measurements made on 42-lb linerboard with varying disk widths are shown in Table II.

TABLE II

SHEAR MODULUS MEASUREMENTS ON RING SAMPLES

Disk Width, mm	Shear Modulus, GPa	Coeff. of Variation, %
6.35	0.0313	18.2
4.76	0.0300	2.6
3.18	0.0262	25.3

These measurements show considerable variability and are lower in magnitude than the mean values of shear modulus summarized in Table I. It is believed that stresses imposed during the mounting and removal of the specimen from the Instron could cause damage to the sample in the form of edge cracking. The polar second moment of area J is given by:

$$J = \frac{\pi}{2} (R^4 - r^4)$$

Where R and r are the outer and inner radius of the disk, respectively. Therefore, if J is in error because of edge cracking, the calculation of shear modulus could also be in considerable error.

Other shear deformation measurements were made using the ring configuration and will be mentioned where appropriate. However, because edge cracking was present it was decided to use a disk type sample. It was also realized that the ring-shaped sample offered no particular advantage over the disk, since ring samples could be cut from the disk after testing. Measurements on disk samples of 42-lb linerboard (no surface preparation) gave an average mean shear modulus of 0.0882 GPa with a coefficient of variation of 8.5%. These values are in better agreement with those in Table I.

Shear Deformation Measurements on Commercial Surface Ground Linerboard and Corrugating Medium

It was anticipated, following the work of Byrd (1) and Fellers (2), that some form of surface treatment, i.e., grinding, would be required to ensure consistent results. It was also of interest to determine how the shear deformation behavior of paper and board might vary in the thickness or z-direction.

A series of 42-lb linerboard and 26-lb corrugating medium sheets were surface ground using the technique developed by Wink (18). Approximately the same amount of

material was removed from the wire and felt sides of the sheet. A technique also was developed for machining samples on a lathe using a vacuum chuck. Ring-shaped samples were symmetrically machined to produce six basis weight intervals. Shear modulus results for these samples are given in Fig. 13. As noted previously, the coefficient of variation is quite large for the ring-type sample. However, the mean shear modulus does not appear to significantly vary with basis weight, i.e., as material is removed. This is consistent with the findings of Fellers (2).

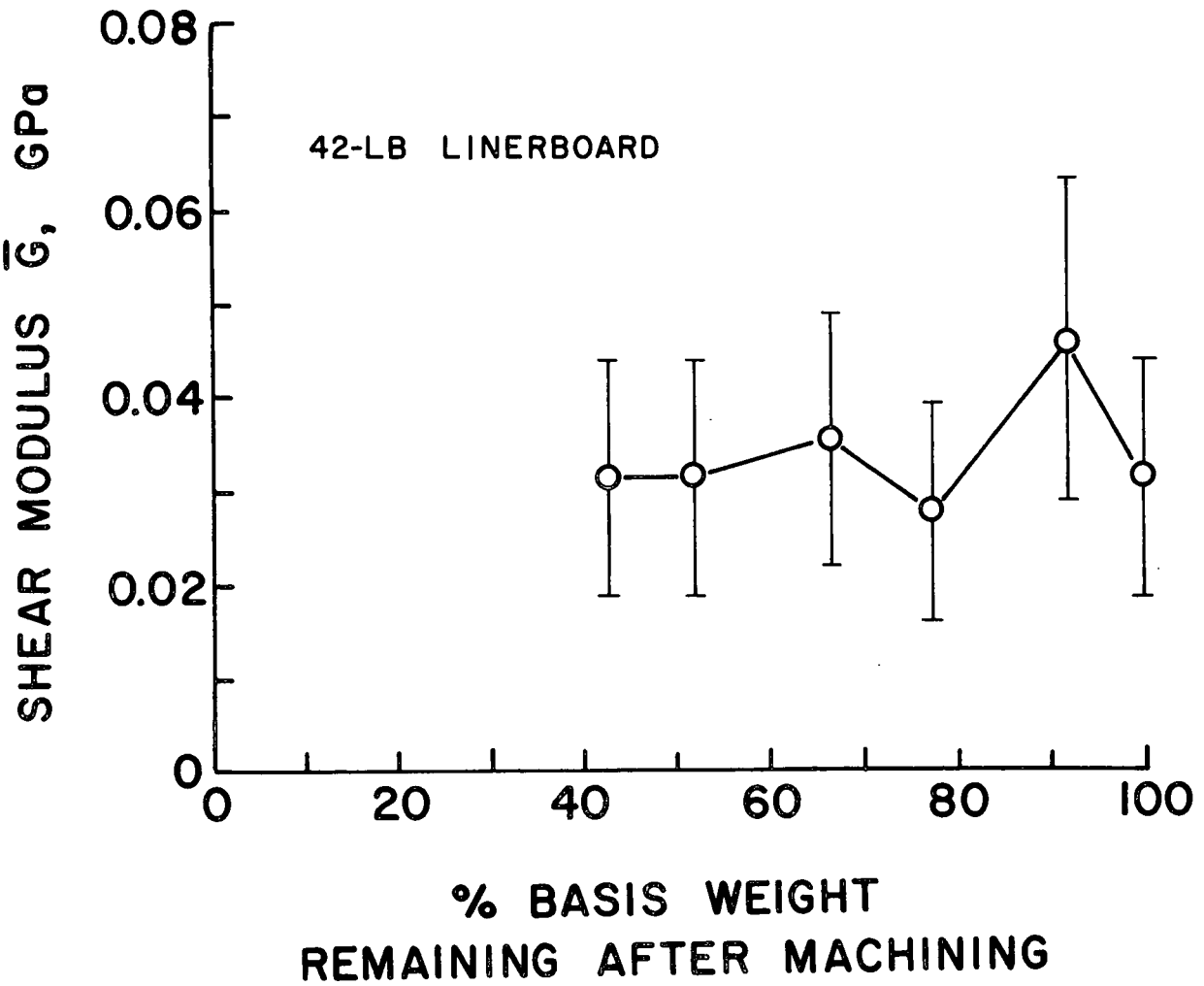

Figure 13. Mean shear modulus variation with basis weight for machined ring samples.

The in-plane and out-of-plane elastic properties determined using ultrasonic techniques for the surface-ground linerboard and corrugating medium sheets referred to above are shown in Fig. 14-17. In these figures, $C_x^2 \doteq E_{MD}/\rho$, $C_y^2 \doteq E_{CD}/\rho$, $(C_xC_y) \doteq \overline{E}/\rho$, $C_{xy}^2 = G_{xy}/\rho$, $V_z^2 = E_{ZD}/\rho$, where E_{MD}, E_{CD}, E_{ZD} are the Young's moduli in the MD, CD, and ZD, respectively, and ρ is the apparent density of the sheet. Also, in Fig. 17, $V_{xz}^2 = G_{xz}/\rho$ and $V_{yz}^2 = G_{yz}/\rho$, where G_{xz} and G_{yz} are the out-of-plane shear moduli in the MD-ZD plane and CD-ZD plane, respectively. The ordinate value on Fig. 17 is obtained by using the geometric mean of the two out-of-plane shear moduli, i.e., $\overline{G} = (G_{xz} \cdot G_{yz})^{1/2}$ $(=\rho(V_{xz}V_{yz}))$. It is interesting to note that for the linerboard and corrugating medium samples, the geometric mean of the in-plane velocities squared decreases with decreasing basis weight while the MD/CD ratio, $R = C_x^2/C_y^2$, increases.

A similar trend is in evidence for the out-of-plane velocities squared as shown in Fig. 16-17. The large change in specific shear modulus at the surface for the corrugating medium may be an artifact associated with surface roughness and is currently under investigation.

Both the linerboard and corrugating medium samples show a reduction in properties (measured ultrasonically) as material is removed. One possible explanation for the variation of in-plane properties is as follows. In-plane longitudinal velocities are quite sensitive to variations in drying stress and fiber orientation. The results suggest that since the orientation ratio R increases and the mean longitudinal velocity squared decreases as material is removed, there must be a significant reduction in drying stress from the surface of the sheet to its interior. A variation in the drying stress in the thickness direction of paper was suggested by the work of Htun and DeRuvo (19), who showed that the overall level of drying stress in paper is controlled by the rate of drying and relaxation processes due to the

viscoelastic nature of paper. It is our intention in future work to measure the variation of drying stress in the thickness direction of paper and to determine its impact on paper properties.

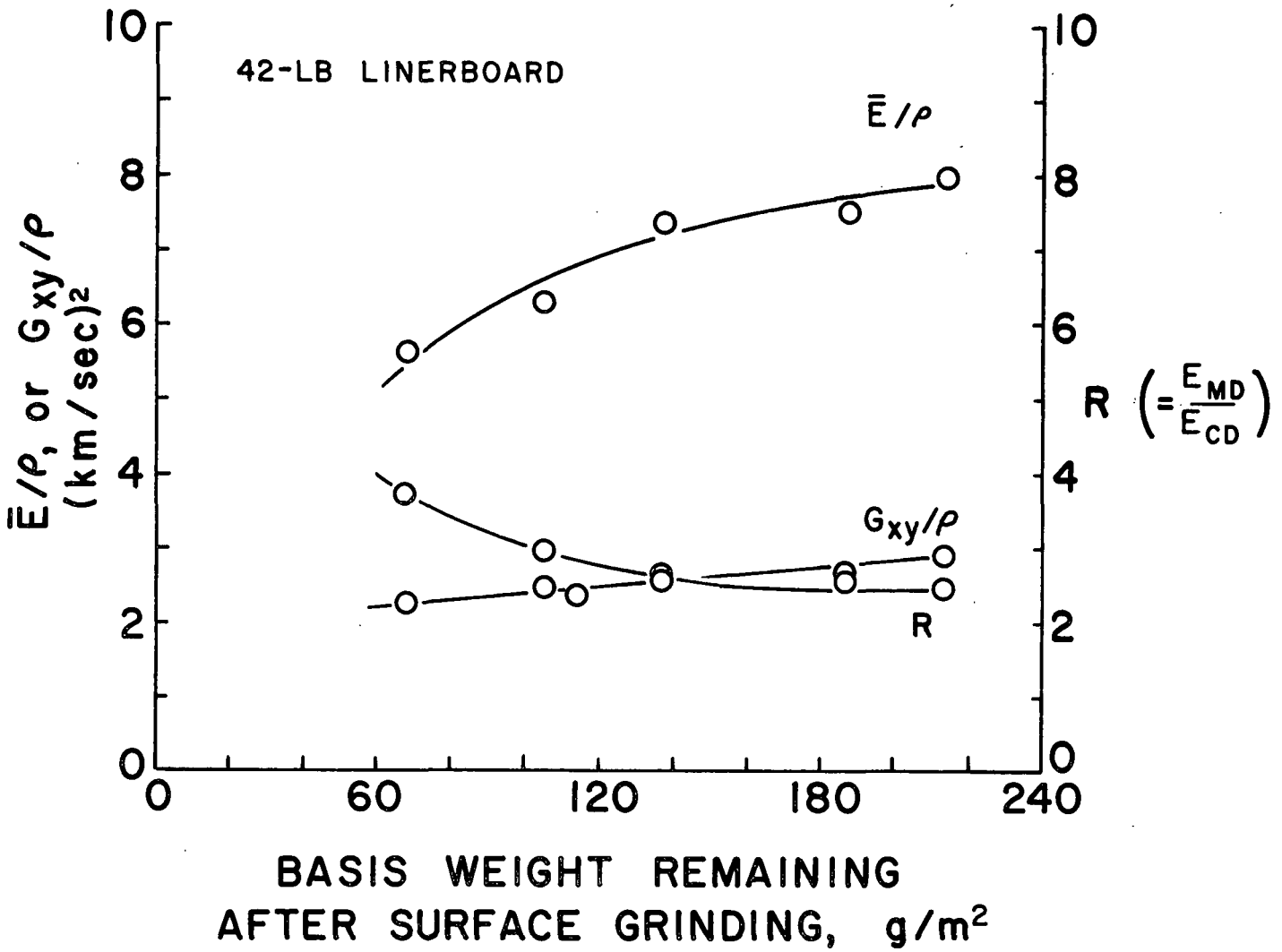

Figure 14. Ultrasonic in-plane property variations with basis weight for ground linerboard samples.

Following characterization of the surface ground sheets, one set was used to prepare a series of disks for mechanical shear deformation measurements. The variation of the apparent mean shear modulus, measured mechanically with the basis weight remaining after surface grinding for the linerboard and corrugating medium samples is shown in Fig. 18. The term "apparent" means that the shear modulus

values have not been corrected for the effects of the mounting tissue or possible adhesive reinforcement of the surface. We will consider these in more detail shortly. We see from Fig. 18 that as material is removed by grinding, there is a slight increase in the linerboard shear modulus (with the exception of the last point) and a more pronounced increase for the medium. A similar behavior was reported by Byrd (1) and Fellers (2), but occurred at a basis weight of less than 50 g/m^2. This trend is opposite to that found with the ultrasonic measurements.

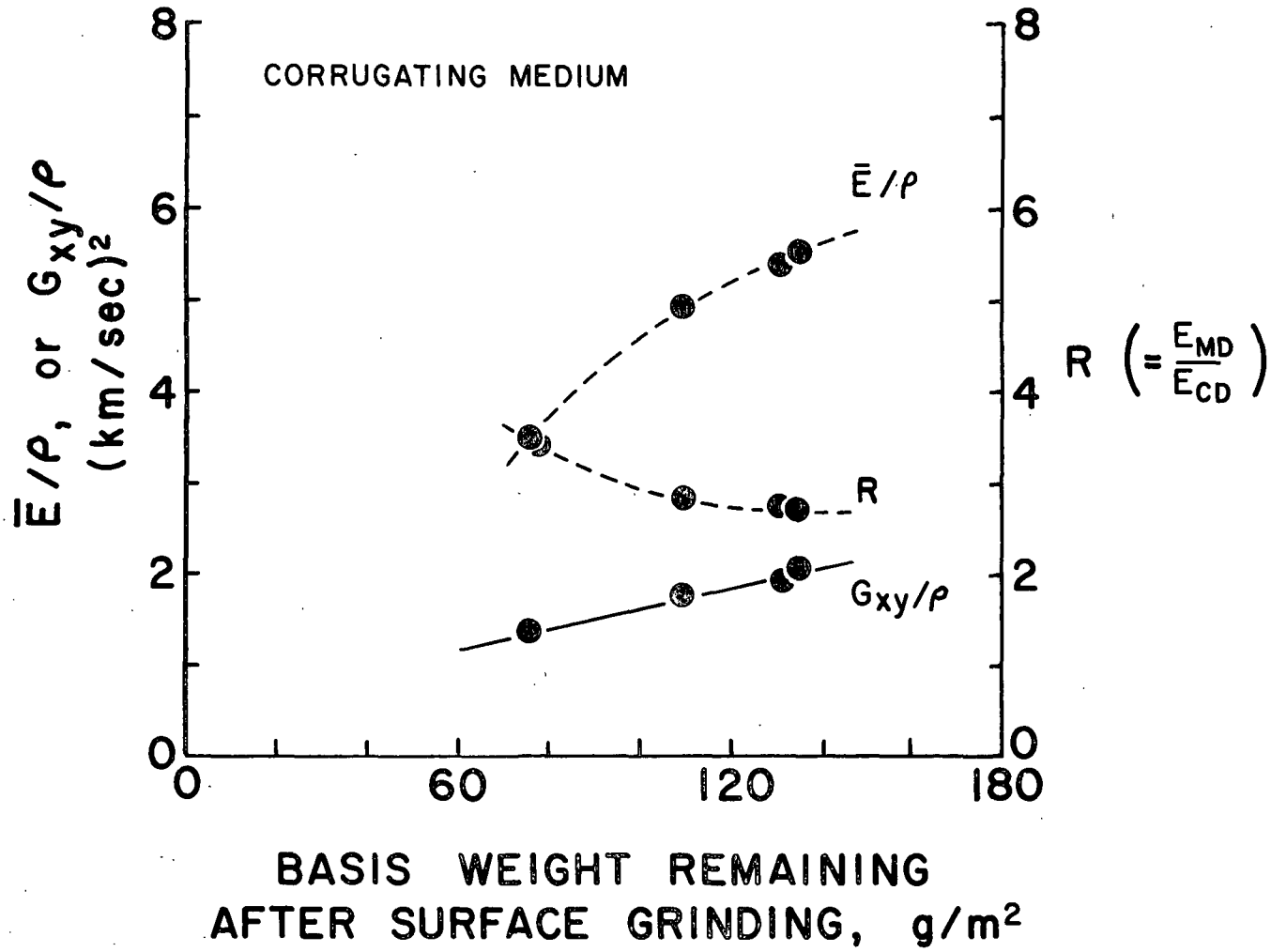

Figure 15. Ultrasonic in-plane property variations with basis weight for ground corrugating medium samples.

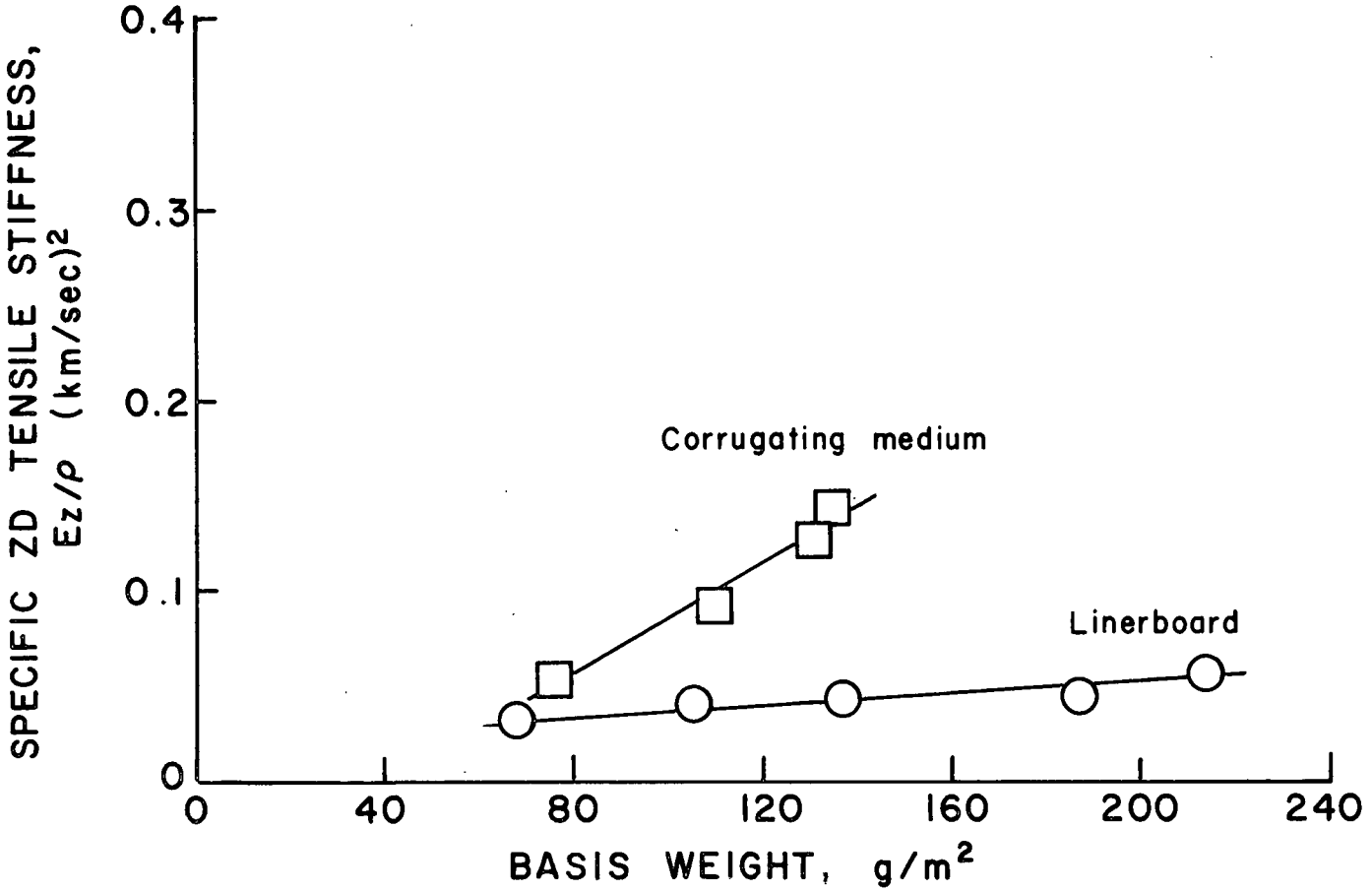

Figure 16. Ultrasonic out-of-plane specific ZD tensile stiffness variation with basis weight for ground samples of linerboard and corrugating medium.

Mounting Tissue Effects

Corrections for the effect of mounting tissue deformation and reinforcement of the outer layers of the sample by the tissue adhesive are given in the Appendix. The corrected values of shear modulus for the linerboard and corrugated medium samples are shown in Fig. 19. With the exception of the lowest basis weight samples, the differences between the uncorrected and corrected values are small. The basic trend is also unaffected. It should be noted that the apparent density of the corrugated medium sample does increase as material is removed by surface grinding (see Table VI, Appendix). This could, in part, explain the increase in shear modulus found with decreasing basis weight. The apparent density of the linerboard, however,

is fairly constant as material is removed by surface grinding (see Table VII, Appendix).

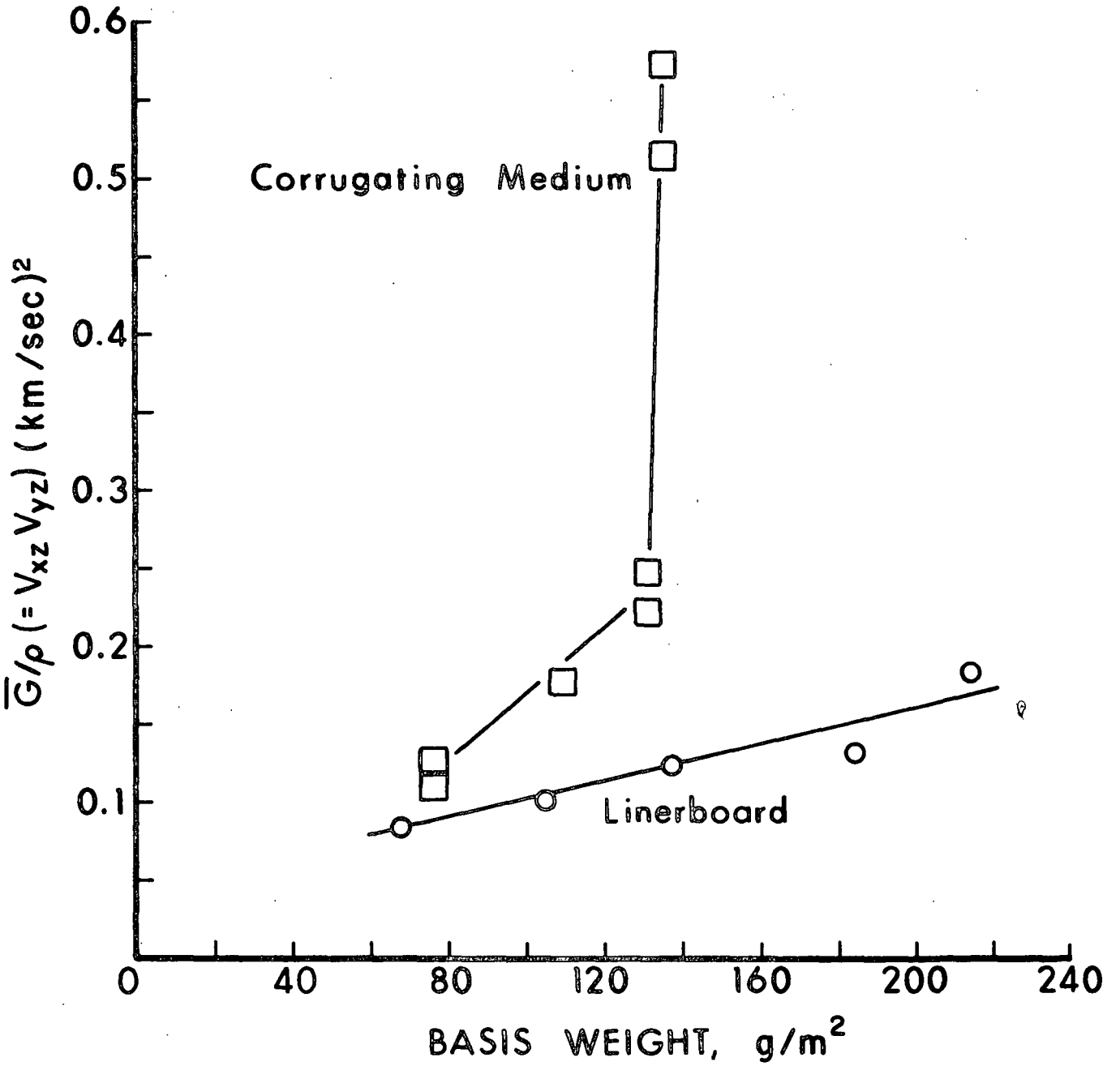

Figure 17. Ultrasonic out-of-plane mean shear modulus vs. basis weight remaining after grinding.

After shear deformation measurements, the linerboard and corrugating medium disk samples were separated from the mounting tissue and mounting cylinders. This

was accomplished by reheating the assembly to a temperature of 120°C for 45 minutes and sliding the cylinders apart. The sample was then slid off the cylinder to which it had remained attached. This procedure leaves a residual layer of adhesive on the samples of approximately constant weight, as shown in Table III. The percentage of the total weight which is adhesive is also shown.

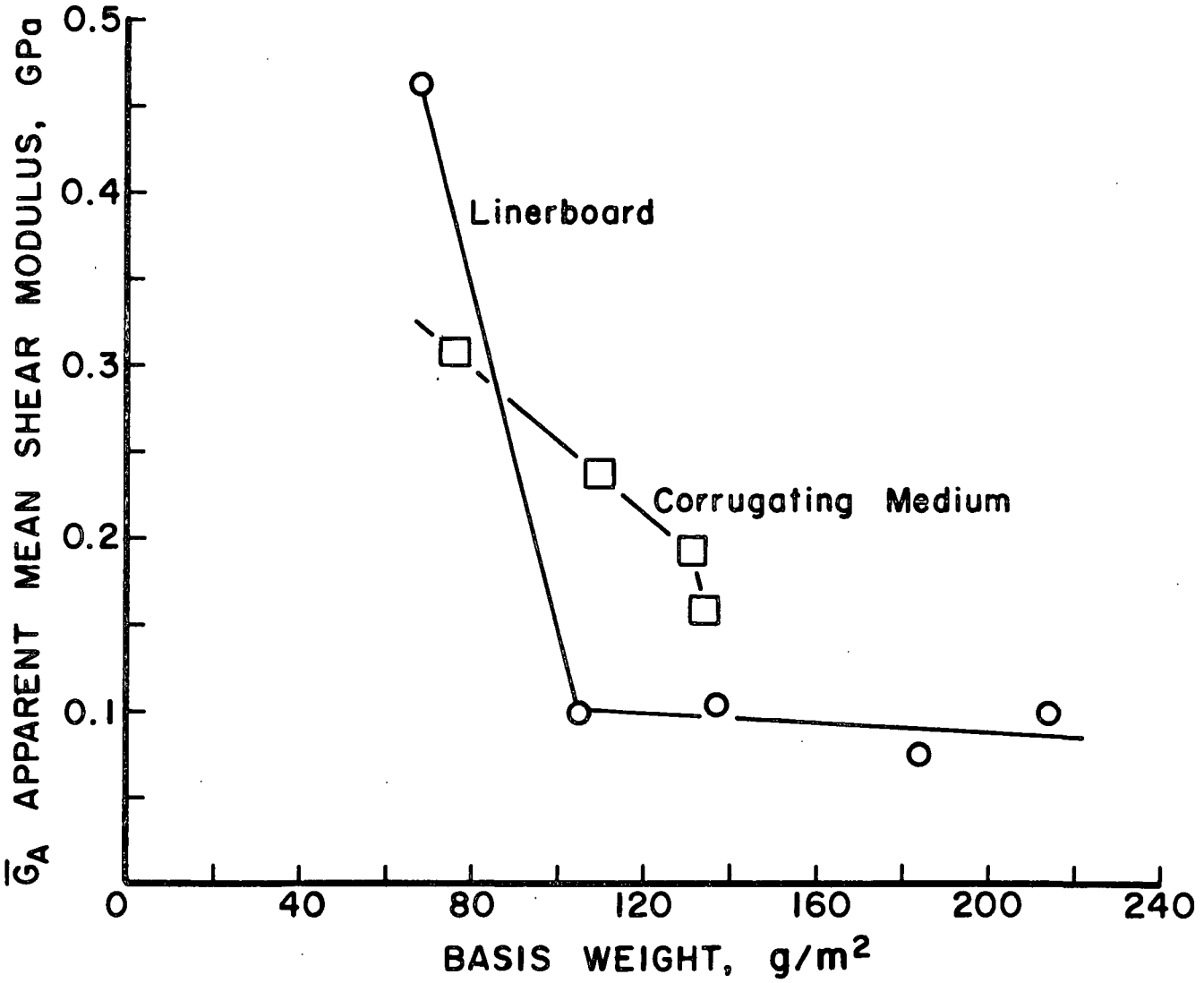

Figure 18. Variation of out-of-plane mean shear modulus measured mechanically with basis weight remaining after grinding for disk type samples.

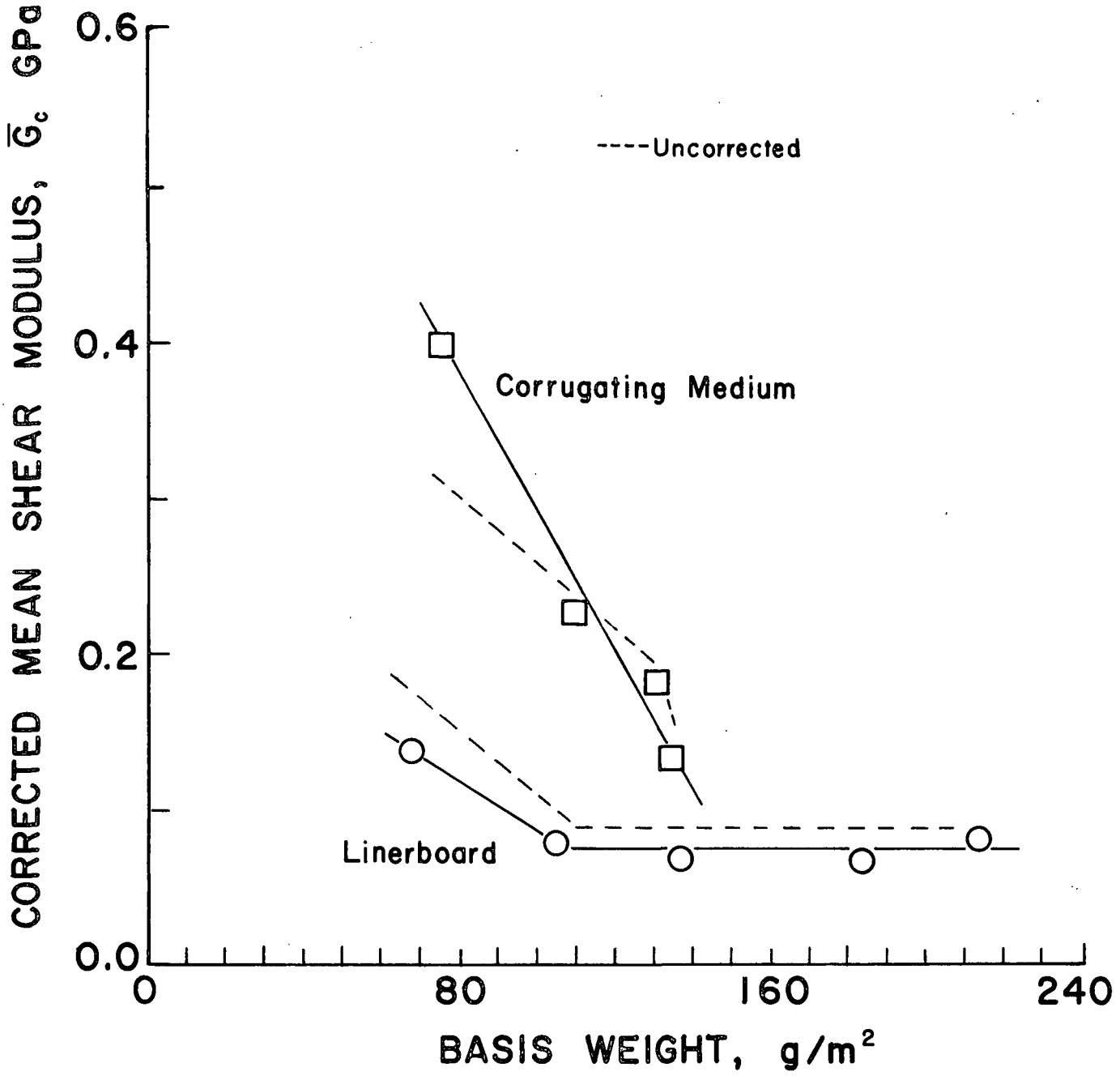

Figure 19. Variation of out-of-plane corrected mean shear modulus determined mechanically with basis weight for ground disk samples.

Ultrasonic shear modulus measurements were also made on these samples. The results for the linerboard are shown in Fig. 20. Values obtained on the actual disk samples before testing (the variation is similar to that shown in Fig. 17 for the

whole sheet) are compared with results for the disks before and after removal of the residual adhesive (using xylene as a solvent). The variation in ultrasonic modulus for the reinforced samples (solid points) is similar to that determined mechanically, as shown in Fig. 18. Furthermore, when the adhesive is removed, the values are in fairly close agreement with the original measurements.

TABLE III

WEIGHT OF MOUNTING TISSUE ADHESIVE ON SAMPLE

Sample No.	Adhesive Wt. gms.	Adhesive, %[a]
L.B. 1	0.0217	8.1
L.B. 3	0.0235	10.2
L.B. 5	0.0209	11.9
L.B. 7	0.0232	16.3
L.B. 9	0.0240	24.0
C.M. 1	0.0139	8.4
C.M. 3	0.0224	13.0
C.M. 5	-	-
C.M. 7	0.0250	22.7

[a]Percent adhesive of sample weight + adhesive.

Samples L.B. 1 and C.M. 1 are not surface ground. This may explain the significant differences in the amount of adhesive retained by C.M. 1 compared with the other C.M. samples.

The more intimate the contact the greater the level of adhesive transferred.

Compressive Strength Measurements on Commercial Surface Ground Linerboard

The in-plane and out-of-plane ultrasonic measurements show a decrease in properties as material is removed by surface grinding. It was therefore important

to determine if this trend could be found in other related properties, particularly compressive strength.

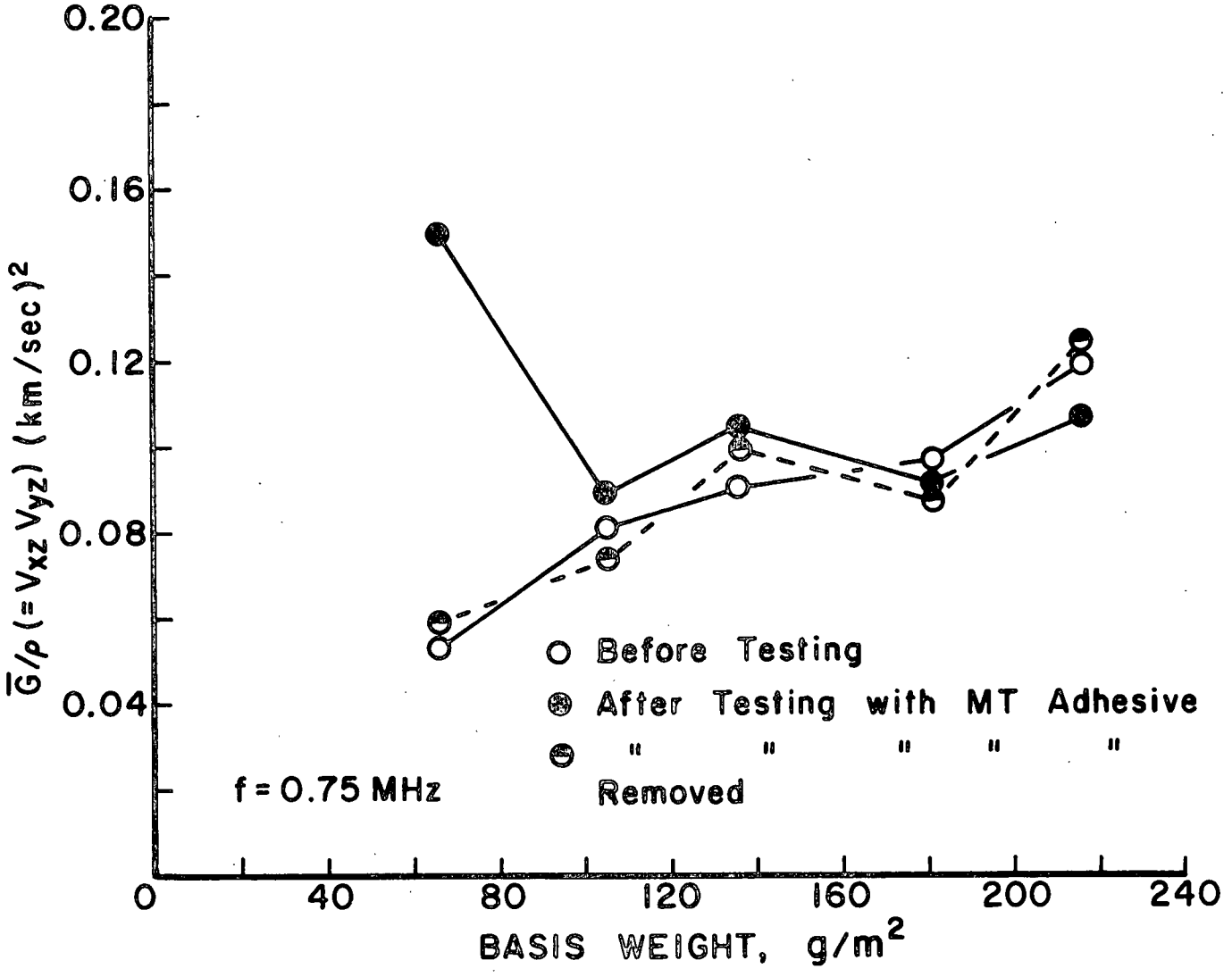

Figure 20. Effects of mounting tissue adhesive on out-of-plane mean shear modulus as measured ultrasonically on disk samples.

STFI compressive strength measurements made on the surface ground linerboard samples are shown in Fig. 21. The open circles are geometric mean values of

MD and CD measurements made on 15-mm-wide strips (standard size). There is a reduction in compressive strength as material is removed by grinding. We might expect a reduction in compressive strength as the span-to-caliper ratio, λ/t, is varied. For the above case the range is $2 < \lambda/t < 7$, which falls within the plateau region of compressive strength as given by Cavlin and Fellers (20) and predicted by Habeger and Whitsitt (21). The decrease in compressive strength is therefore consistent with the change in properties measured ultrasonically.

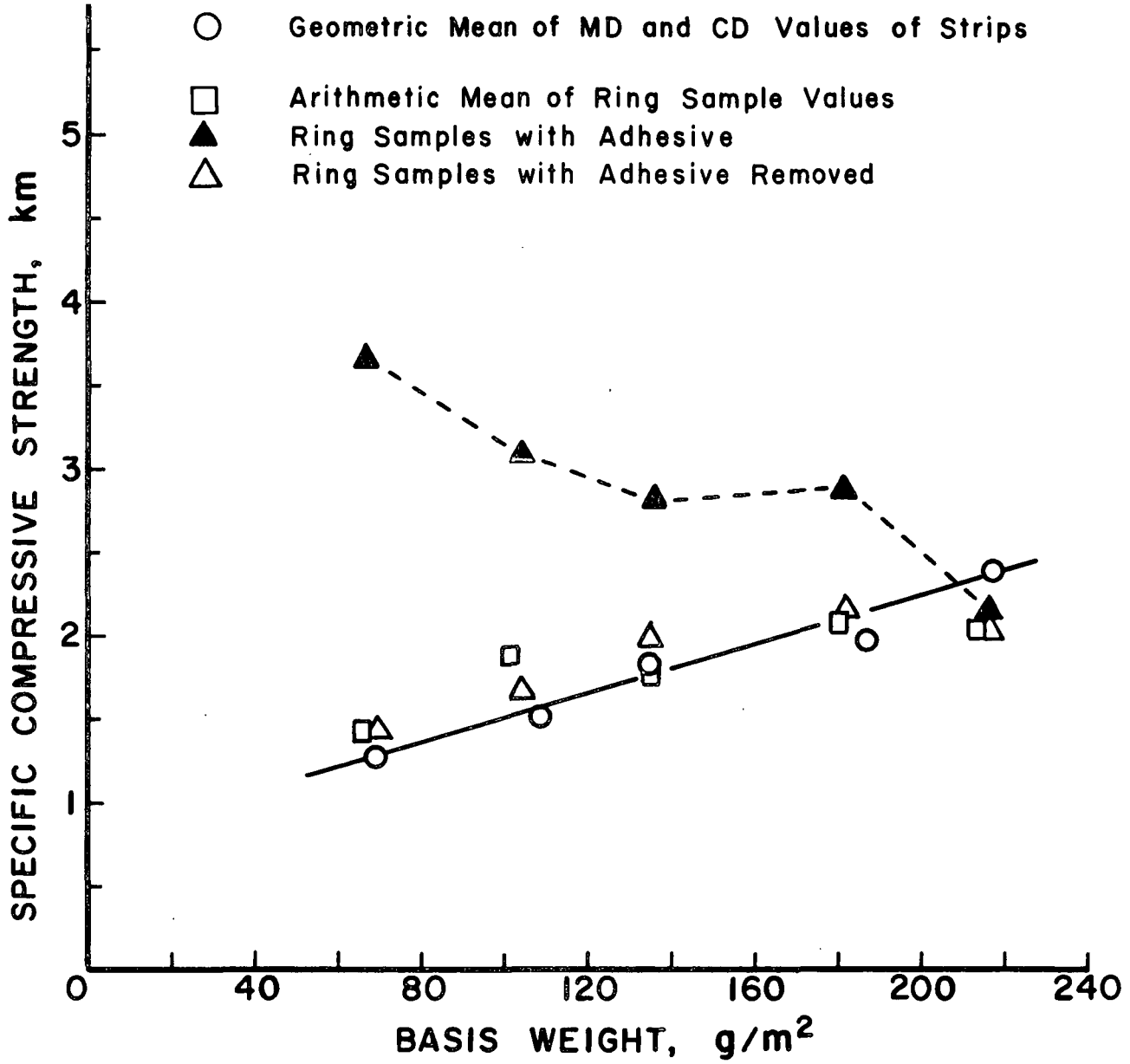

Figure 21. Effects of mounting tissue adhesive on STFI compressive strength on surface ground linerboard.

Also shown in Fig. 21 are compression measurements made on ring type samples punched from the disk samples. Compressive measurements are made at the positions shown in Fig. 22.

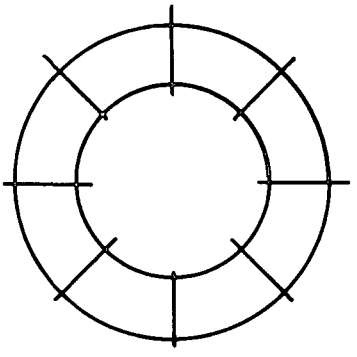

Figure 22. Location of compression measurements.

The arithmetic means of these values are shown in Fig. 21. There is basically good agreement between compressive strength values measured on strips and those measured on the ring samples. The solid triangles are the measurements made on samples after their mechanical shear modulus has been determined and before the mounting tissue adhesive is removed. We see that the effect of adhesive reinforcement has a very significant impact on compressive strength and, furthermore, when this adhesive is removed, the values (open triangles) are essentially in agreement with the controls.

A similar behavior for the effects of adhesive reinforcement was also found for machined ring samples (see Fig. 23). In this case the disks were removed from the mounting cylinders using xylene after the mechanical determination of shear modulus. In-plane ultrasonic velocity measurements were also made on these ring sample disks and their mean squared values are shown in Fig. 24. Again, there is a significant increase in in-plane stiffness due to adhesive reinforcement. The variation is consistent with the variation found for compressive strength.

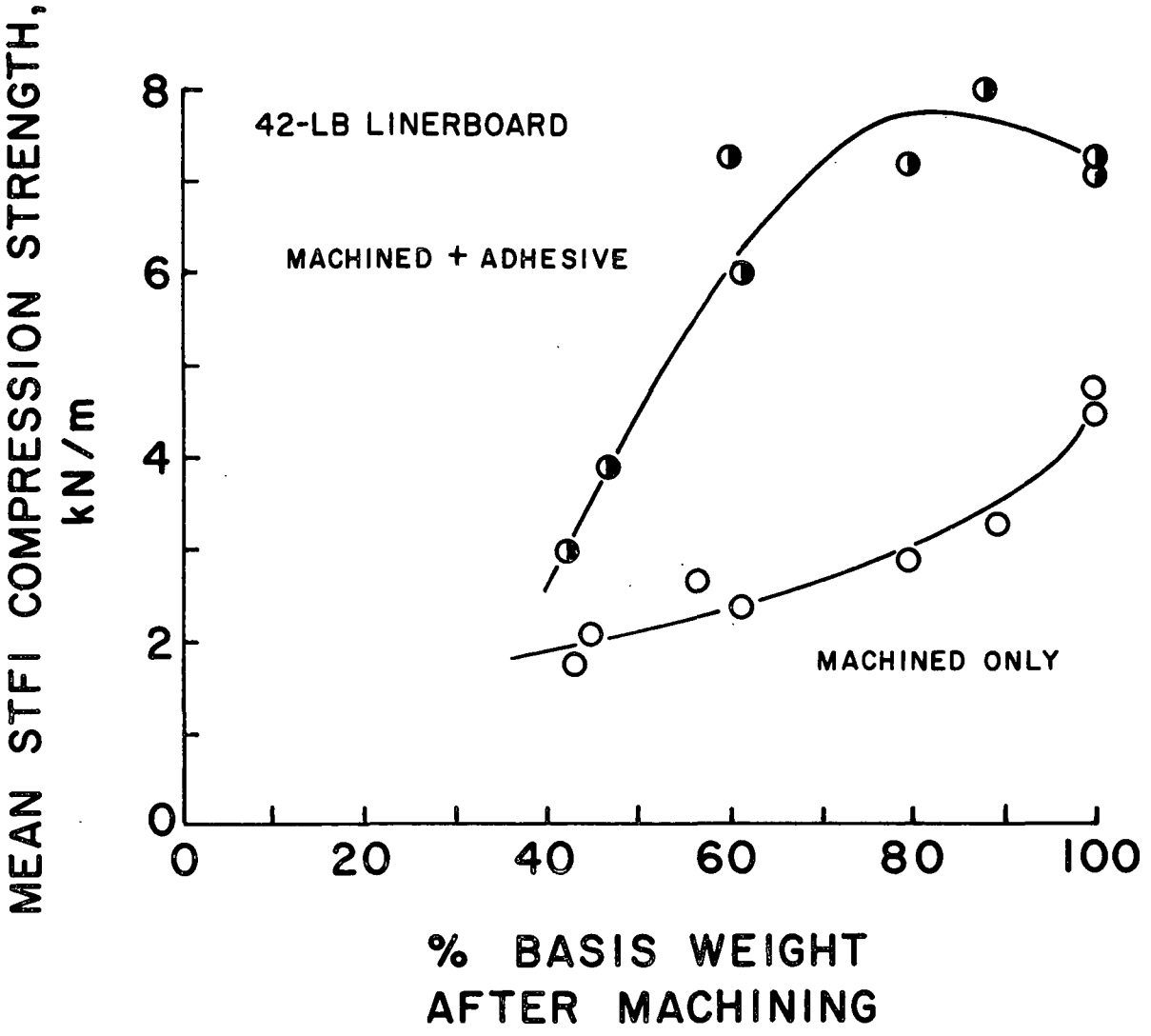

Figure 23. Effects of mounting tissue adhesive on STFI compression strength measurements on ring samples of machined linerboard.

The variation in compressive strength as material is symmetrically removed by surface grinding or machining leads one to ask what differences might be found for the wire and felt sides of the sheet? The results for a series of machined disks are shown in Fig. 25. As might be anticipated from conventional wisdom, the felt side compressive strength values are higher than those of the wire side, whereas the middle section is lower than either one.

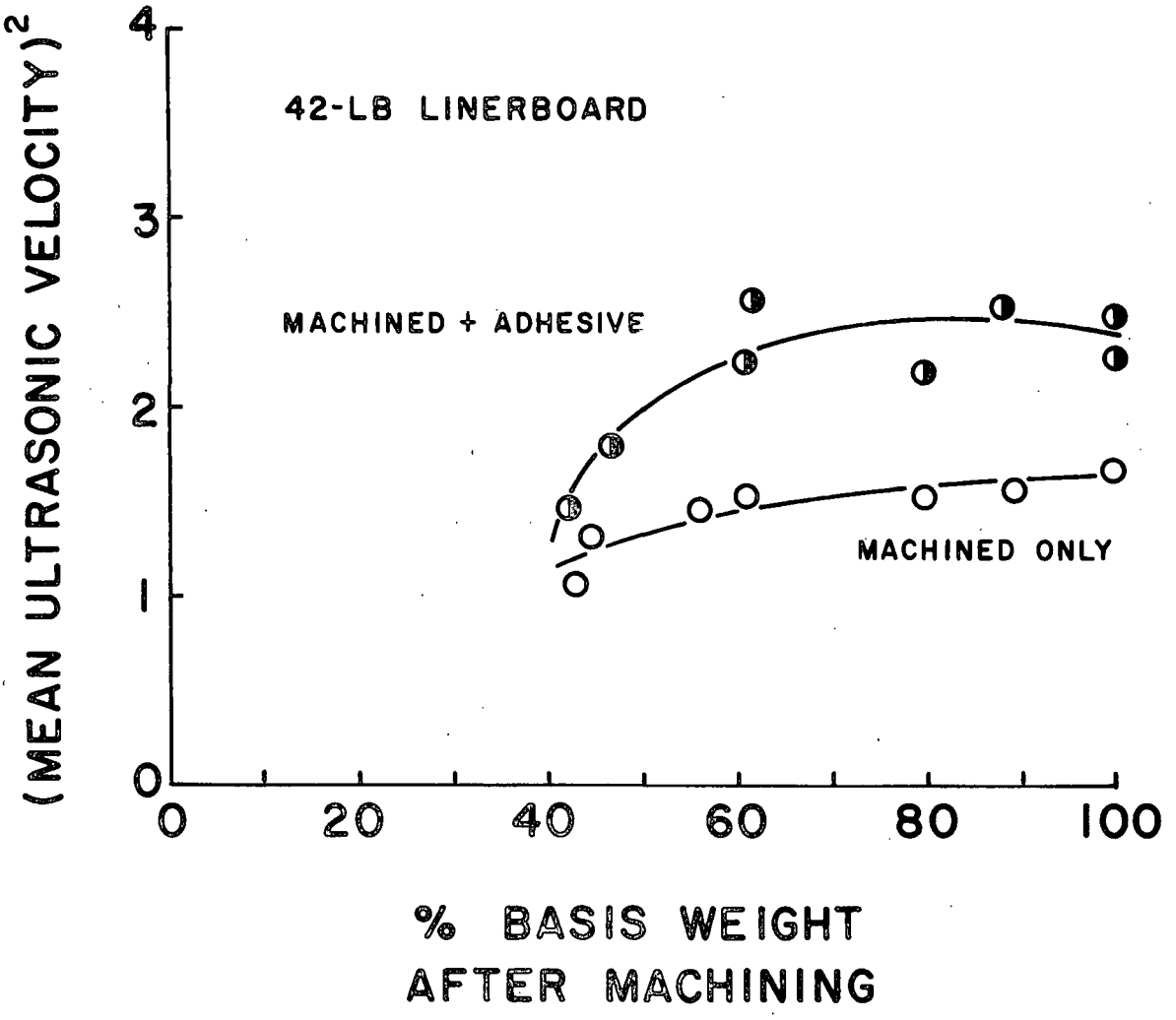

Figure 24. Mean in-plane longitudinal $(velocity)^2$ variations with basis weight on ring samples.

The above findings for compressive strength behavior are consistent with both the in-plane and out-of-plane ultrasonic measurements, indicating a significant variation in properties in the thickness direction of paper.

Effects of Basis Weight and Drying Conditions on Shear Deformation Behavior - Oriented Handsheets

Oriented handsheets were made on the Dynamique Formette. The sheets had a nominal basis weight of 50, 100, 150, and 200 g/m^2 and were formed from an unbleached

softwood kraft pulp having a 475 CSF. One half of the sheet was removed and dried without restraint. The other half was dried with restraint. Even though the unrestrained sheets were dried slowly, some wrinkling occurred. The results of in-plane and out-of-plane ultrasonic measurements are shown in Fig. 26. The elastic constants are greater for the restrained condition (r), as might be expected. We also see some variation with basis weight.

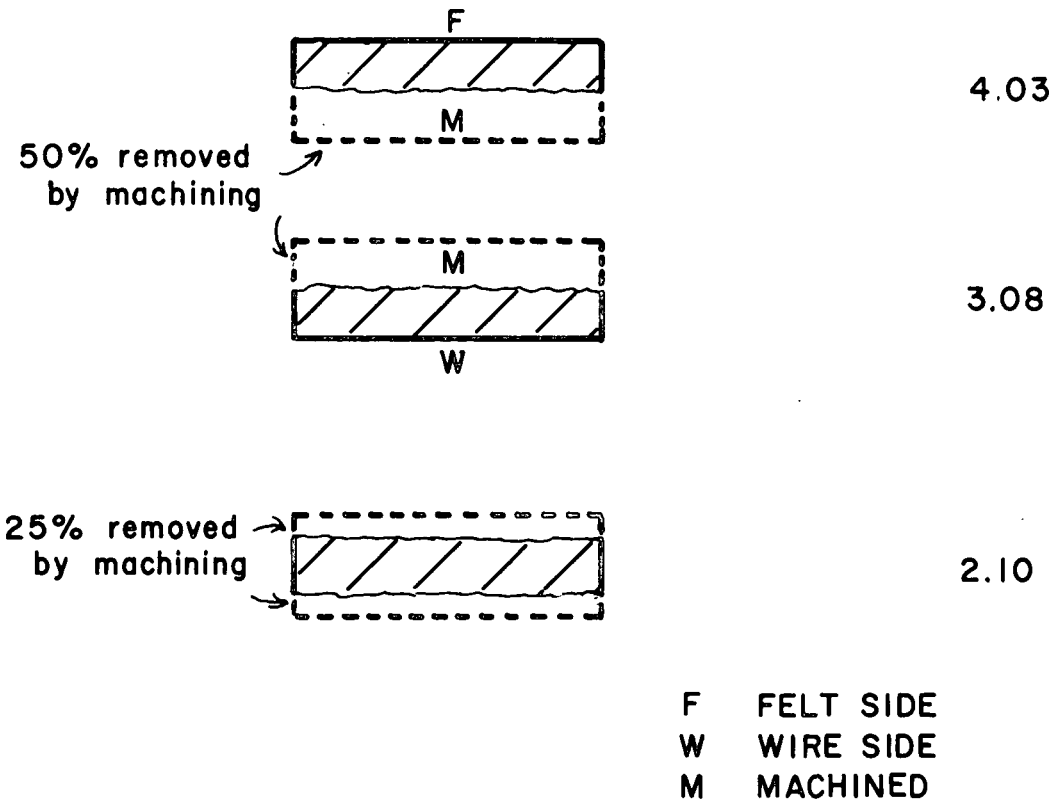

Figure 25. Effect of material removal by machining on compressive strength of linerboard.

An attempt was made to maintain a constant apparent density by varying the conditions of wet pressing. However, we see in Fig. 27 a significant variation in apparent density with basis weight as determined using standard TAPPI caliper

measurements. In contrast, the apparent density calculated using IPC soft platen caliper measurements (22) shows less variation in density.

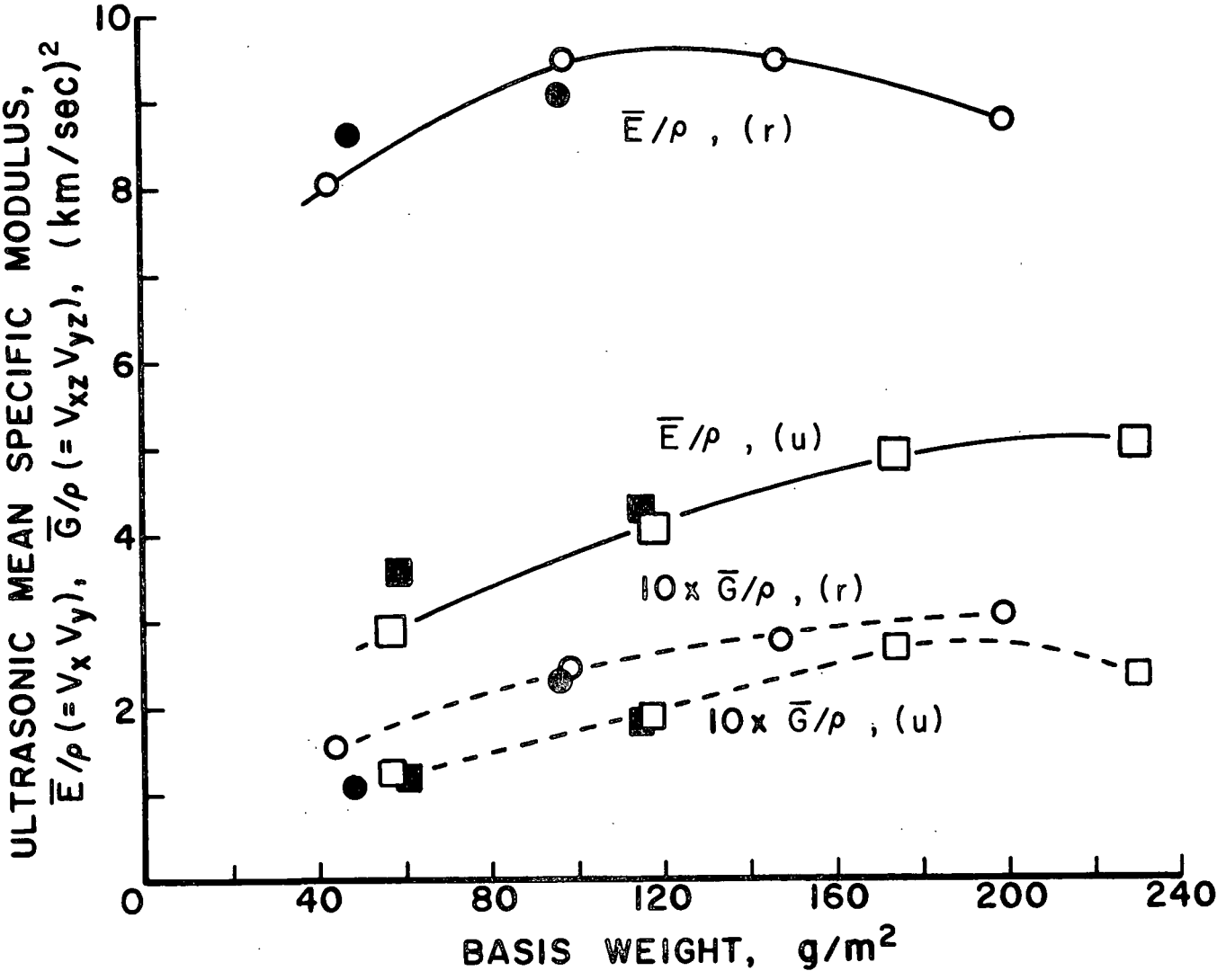

Figure 26. Ultrasonic specific moduli for Formette handsheets; (r) means the sheet was restrained, (u) means the sheet was unrestrained.

In view of the literature (11,12), and as previously discussed, it was expected that the restrained sheets would yield a higher density based on TAPPI caliper measurements. However, using the soft platen technique the opposite effect is found; i.e., the unrestrained sheets have slightly higher density values. We have not yet made bonded area and IPC apparent density (soft platen) measurement

comparisons, but we speculate that a good correlation will be found. On this basis we believe that the higher density values of the unrestrained sheets are consistent with slightly higher levels of bonding. Page and Seth (23) at PPRIC have found that measurements of scattering coefficient on freely dried and restrained sheets are almost identical.

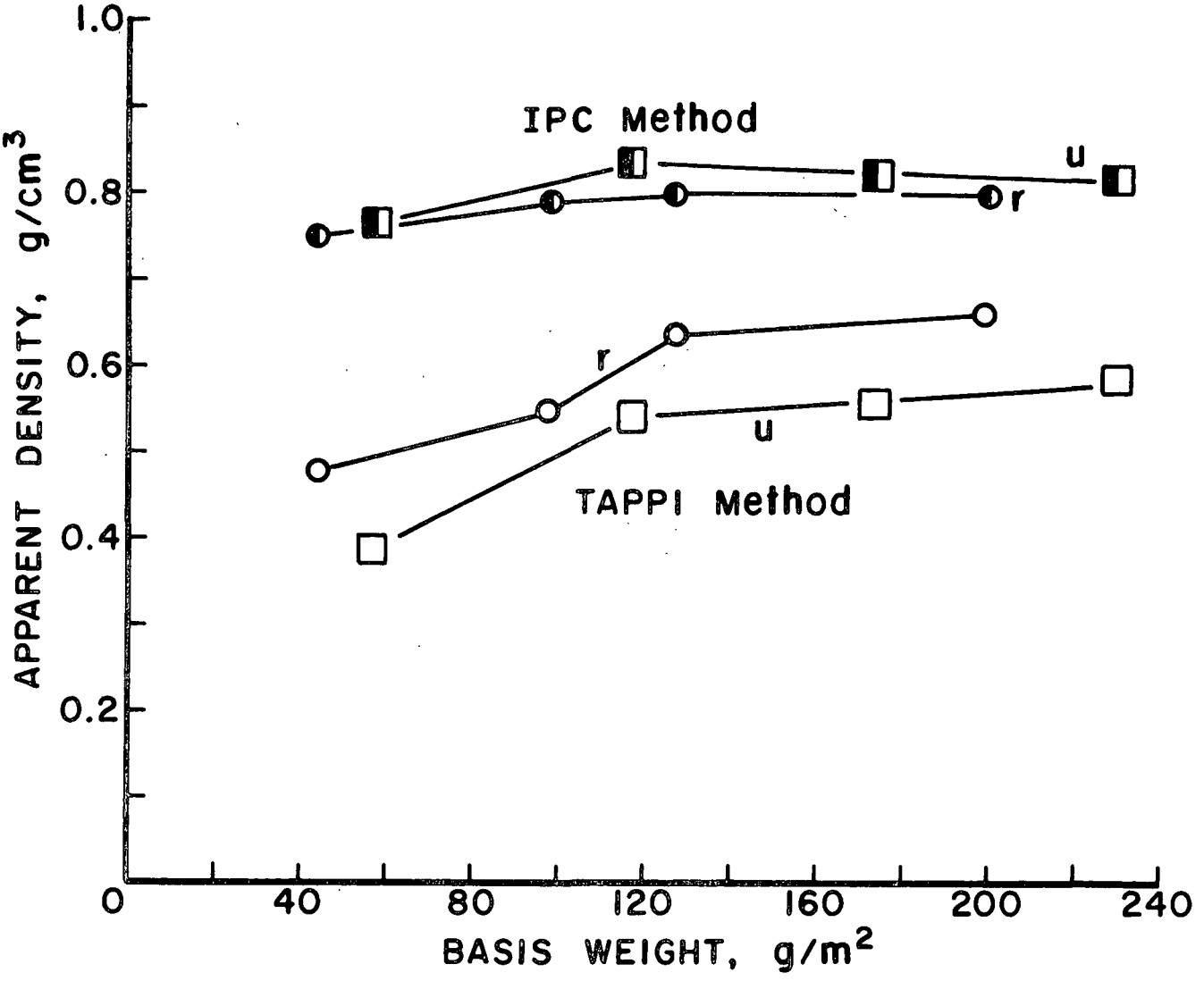

Figure 27. Apparent density measurements on Formette handsheets.

The variation in in-plane constants is believed to be due to variations in drying restraint, and we see in Fig. 26 that the in-plane elastic constants of the freely dried sheets (u) also show a significant variation with basis weight. This

perhaps implies that the rate of drying is varying with basis weight and even in the absence of restraint there will still be a significant difference in the level of internal stress and hence elastic constants.

The out-of-plane mean specific shear modulus is greater for the restrained dried sheets than the unrestrained sheets, as shown in Fig. 26. These results should be compared with the mechanical measurements of mean shear modulus and strength shown in Fig. 28-29. No surface preparation, i.e., surface grinding or machining, was performed on these latter samples. It may be for this reason that the results are somewhat more erratic than previous results. Nevertheless, we see that the values of modulus and strength for the unrestrained sheets are somewhat higher than for the restrained sheets. This is also consistent with the higher values of apparent density (IPC) found for the freely dried sheets. These results are similar to those reported by Byrd (6), who has also investigated the effects of drying restraint on shear deformation behavior.

Compressive Strength Measurements - Oriented Handsheets

The effects of drying restraint conditions on compressive strength for the Formette sheets are shown in Fig. 30. The higher values of compressive strength for the sheets dried under restraint are mainly attributed to their higher in-plane elastic constants.

The Effects of Shear Deformation on Compressive Strength

In the fluting process the medium is subjected to a variety of stresses, e.g., tensile, compressive, bending, and shear, which may affect its properties. Whitsitt and Sprague (9) have investigated bending stresses and found them to have an adverse effect on the compressive strength of the medium. In this investigation

we have tried to determine the influence of shear deformation on the subsequent compressive strength of the medium.

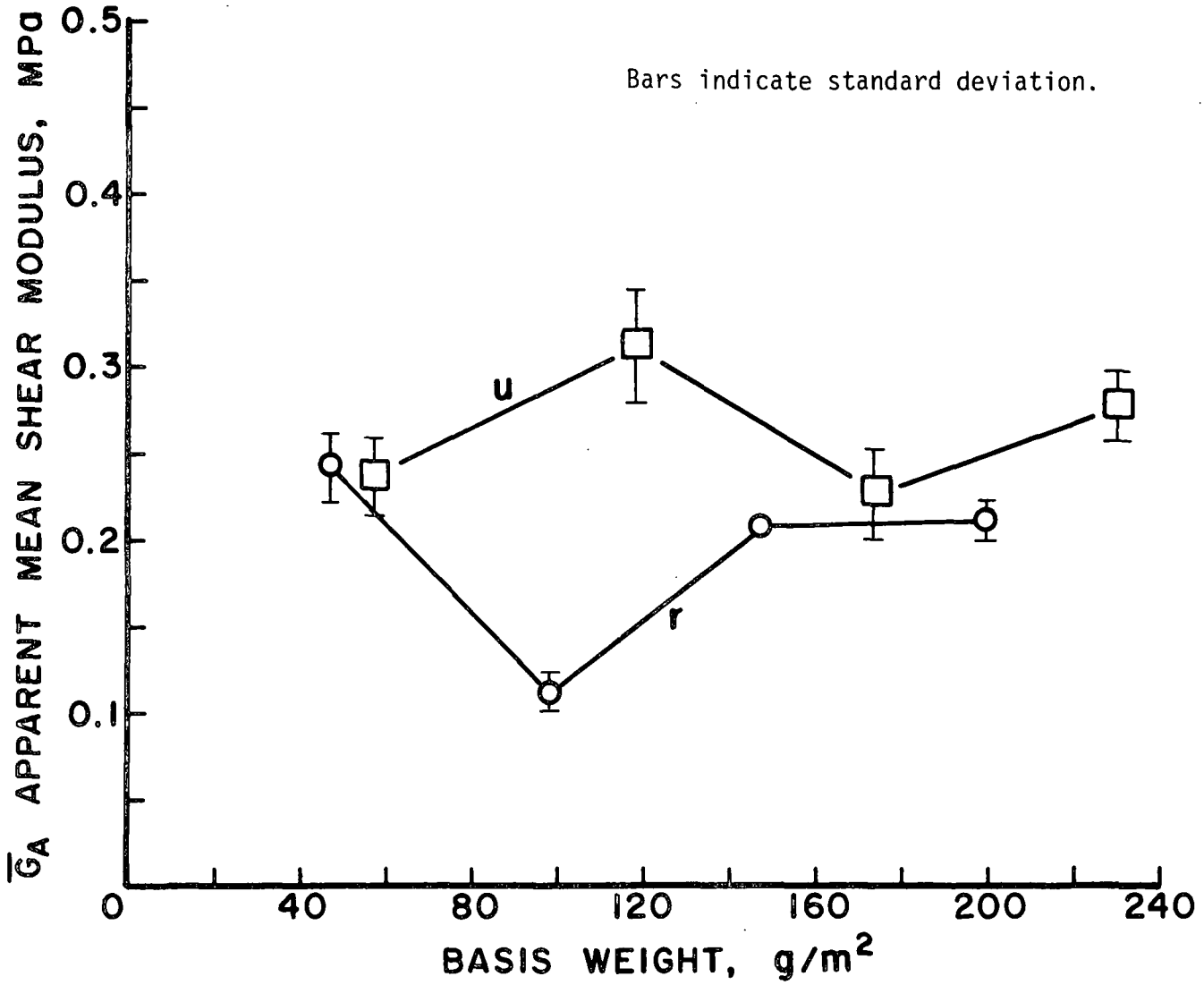

Figure 28. Mechanical shear modulus measurements - Formette handsheets.

Using the techniques already described, disks were cut from samples of commercial medium. After mounting and conditioning, the disks were subjected to varying levels of shear strain up to failure. A typical torque/angular deformation curve to failure is shown in Fig. 31. The inset shows a lower level of applied strain; the initial part of the torque/angular deformation curve after the first strain cycle

has been offset for clarity. From such curves both the initial shear modulus and the modulus after strain cycling could be determined. The disks were then carefully removed from the mounting cylinders and any adhesive remaining was removed using xylene. Ring samples were then cut from these disks to determine the compressive strength as previously described.

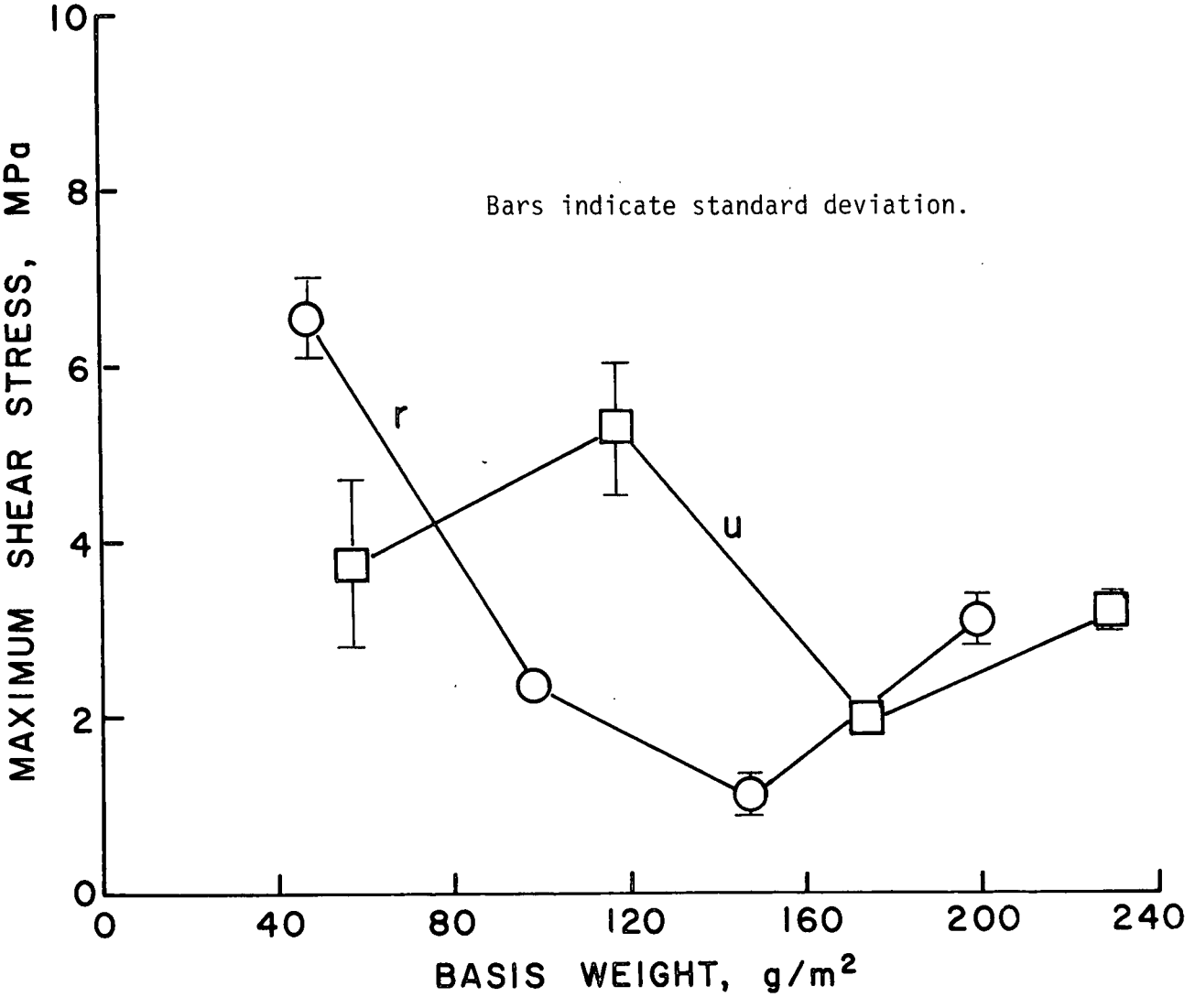

Figure 29. Maximum shear stress measurements - Formette handsheets.

Table IV summarizes the shear modulus and compressive strength data together with ultrasonic measurements of shear modulus made before and after mechanically strain cycling. A considerable variation in shear modulus is noted compared

with that determined in earlier measurements. The difference is attributed to the fact that these measurements were made using the Instron chucks (see experimental section) and not the pin mounting used in earlier work, and sample surface roughness effects.

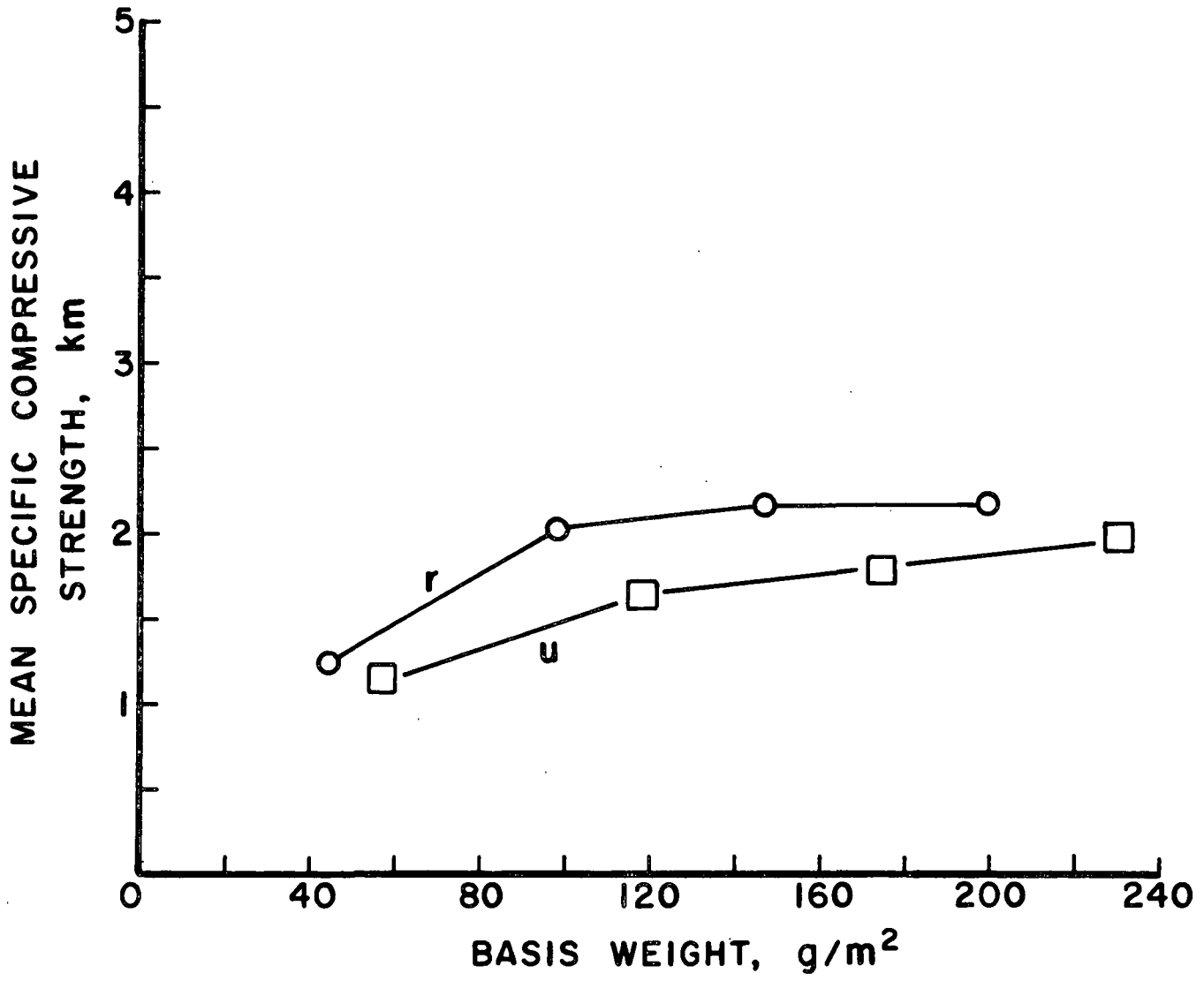

Figure 30. Mean (STFI) compressive strength measurements - Formette handsheets.

The compressive strength vs. initial shear strain results are shown in Fig. 32. No reduction in compressive strength is found with increasing levels of applied shear strain. The variation of specific shear modulus determined ultrasonically

with initial mechanical shear strain is shown in Fig. 33. At high strain levels we see a reduction in shear modulus. This implies that the weak zones for shear failure are not necessarily those for compressive failure. It also means that pure shear deformation may not have the adverse effect on compressive strength that Whitsitt and Sprague (9) found for bending stresses. However, shear in combination with bending may result in a greater reduction in compressive strength than that found with bending alone.

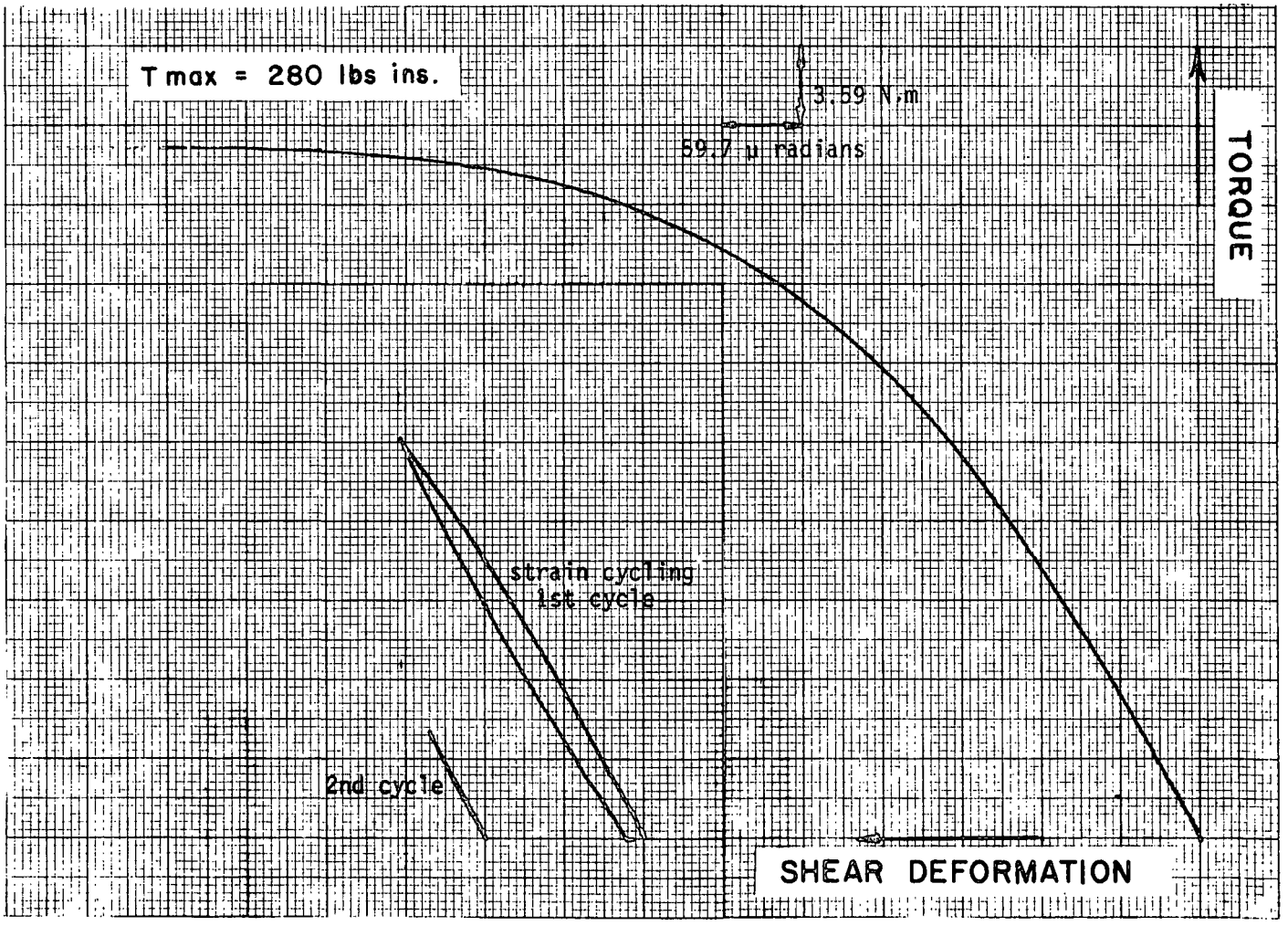

Figure 31. Shear deformation behavior - torsion mode Instron.

TABLE IV

PROPERTIES OF COMMERCIAL CORRUGATING MEDIUM

Sample No.	Caliper, inch	Initial Shear Strain, %	$\overline{G}_i$, GPa	$\overline{G}_f$, GPa	σ_c, Nm/g	$(\overline{G}/\rho,)_i$ $(km/sec)^2$ 0.7 MHz	$(\overline{G}/\rho,)_f$ $(km/sec)^2$ 0.7 MHz
1 F	0.0112	0.60	--	--	25.3	0.733	0.369
2 G	0.0108	0.45	0.187	0.194	22.1	0.455	0.225
3 H	0.0108	1.28	0.151	0.153	26.5	0.506	0.501
4 I	0.0113	--	--	--	--	0.383	--
5 A	0.0110	1.21	--	--	27.0	0.319	0.385
6 B	0.0107	2.08	0.131	0.127	25.8	0.358	0.472
7 C	0.0109	2.49	0.0946	0.0926	26.0	0.340	0.294
8 D	0.0106	3.86	0.0881	0.0780	22.5	0.405	0.194
9 E	0.0109	5.31	0.148	--	25.4	0.413	0.176
10 J	0.0107	4.70	0.0688	0.0603	27.8	0.323	0.162
Controls							
C-1					23.3		
C-2					23.9		

Previous evaluation of corrugating medium gave $\overline{G}_i$ = 0.157 GPa with a coefficient of variation = 6.4%.

Out-of-plane shear (ultrasonic) and compressive strength measurements were also made on the Formette handsheet samples previously discussed, after they had been mechanically tested to failure in shear. The results are shown in Table V. This table does not include results for samples which had separated into two halves. Shear failure is evidenced by a dramatic decrease in shear modulus (whether or not the adhesive layer is present). However, as with the corrugating medium results

discussed above, the straining of the samples to failure does not appear to have a significant effect on compressive strength.

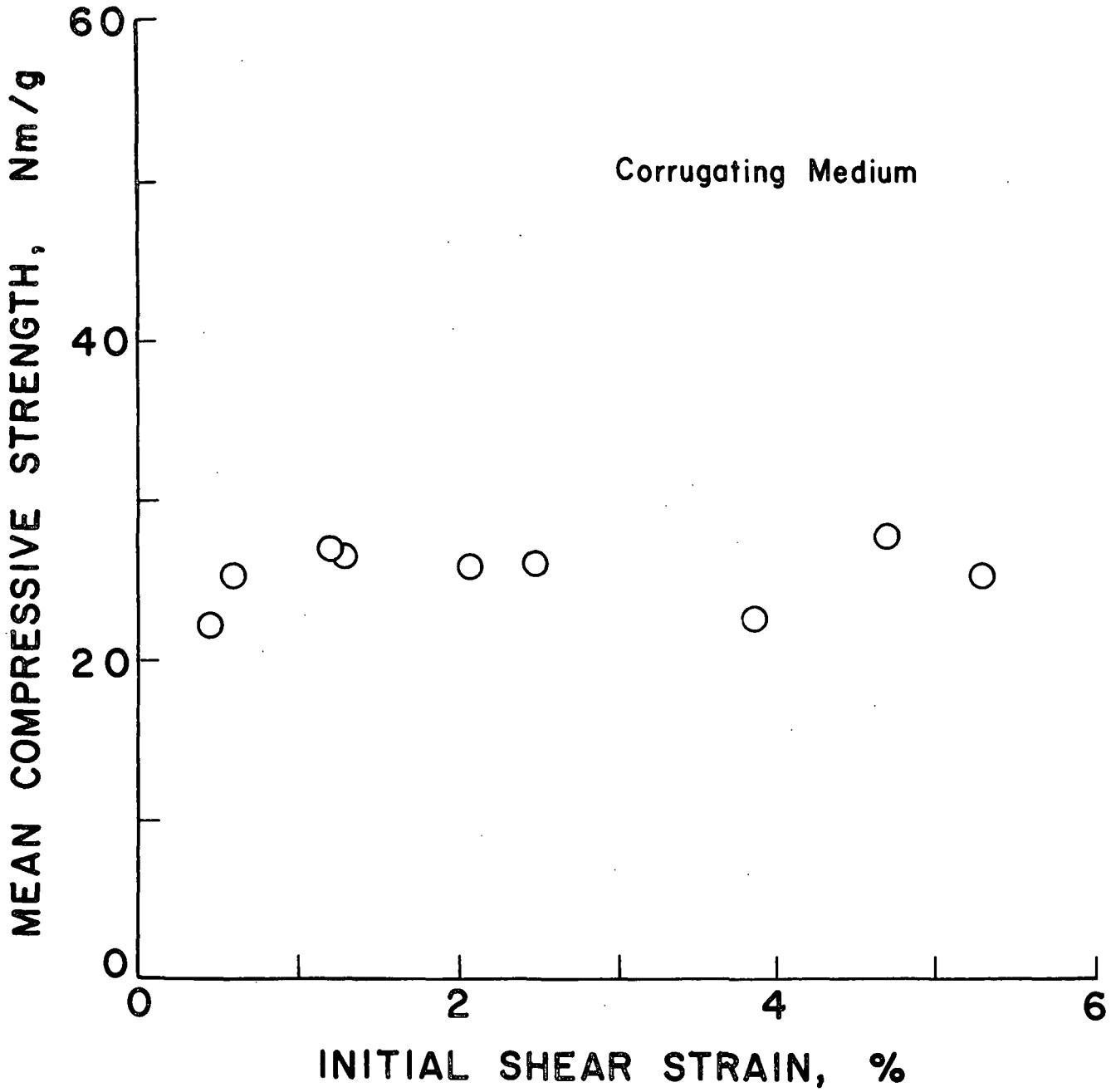

Figure 32. Effect of mechanical shear straining on mean compressive strength.

Failure Mode in Shear - Oriented Handsheets

The failure mode in shear was investigated using light microscopy and SEM techniques. The sample disks chosen were samples which had been previously characterized by ultrasonic methods and mechanically sheared to failure. The oriented

handsheets were made on the Formette (see Page 19), and one set was dried with full restraint (designated 100 r) and the other without restraint (100 u). The properties of the samples selected for this investigation are summarized in Table VI. Note that the shear modulus and shear strength are greater for the unrestrained sheet than for the restrained sheet.

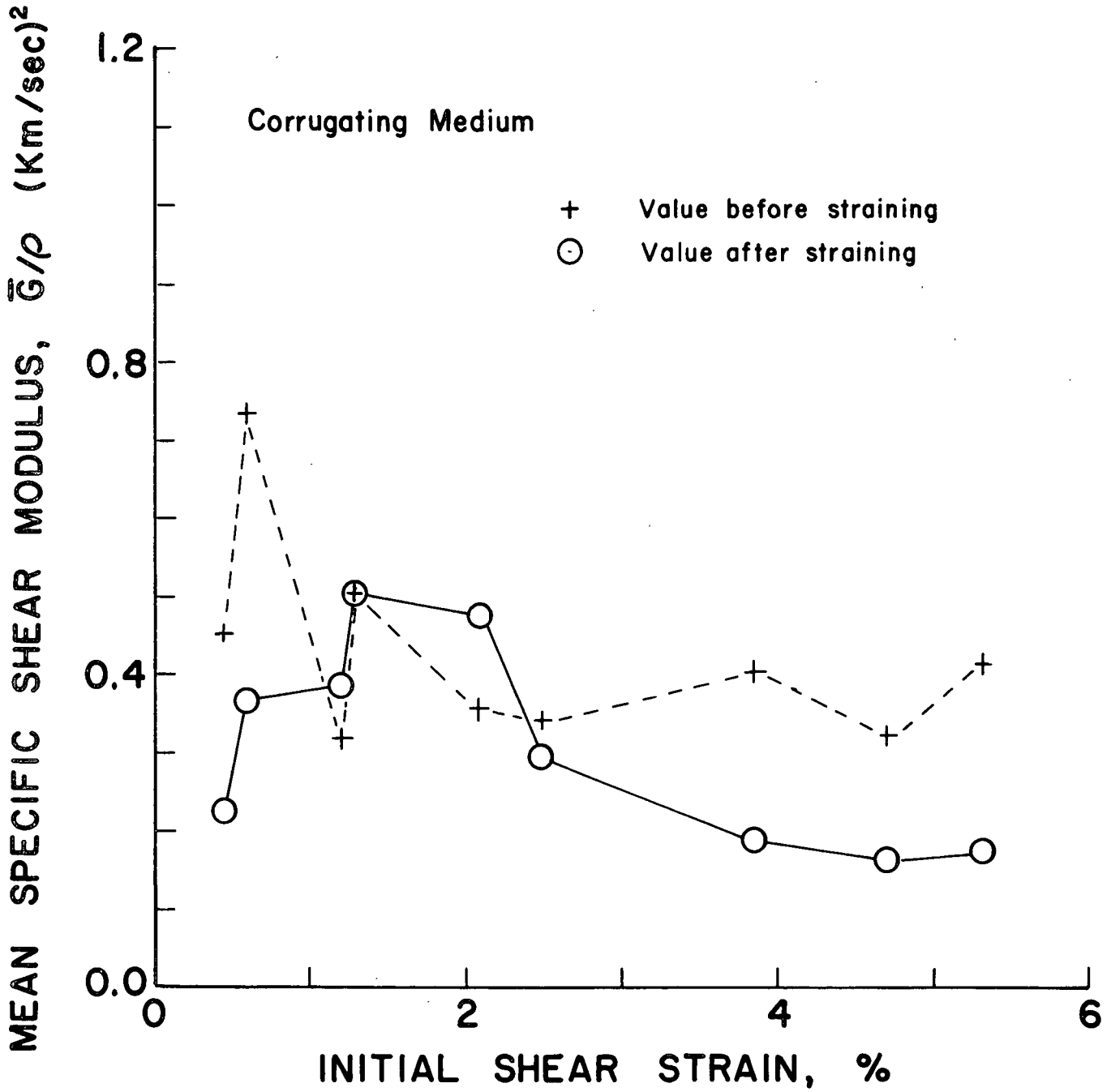

Figure 33. Effect of shear straining on ultrasonic specific shear modulus measurements on disk samples.

TABLE V

MODULUS AND STFI COMPRESSION MEASUREMENTS ON FORMETTE HANDSHEETS

No.	Initial Value $\frac{\overline{G}^a}{\rho}$	After Testing to Maximum Shear: With Adhesive Layer $\frac{\overline{G}^a}{\rho}$	After Testing to Maximum Shear: Adhesive Removed $\frac{\overline{G}^a}{\rho}$	Adhesive Before Removal, %	Initial Specific Compressive Strength, km	After Testing To Failure Specific Compressive Strength, km
200 r	0.2214	0.055	0.056	7.70	21.3	23.6
150 r	0.1913	0.0436	0.0464	9.73	21.2	18.5
100 r	0.1396	0.0264	0.318	15.3	19.8	19.1
50 r	0.0538	--	--	--	12.1	--
200 u	0.2315	0.055	0.0749	5.29	19.3	20.0
150 u	0.0809	0.0451	0.0569	7.33	18.5	17.7
100 u	0.0809	0.0223	0.048	12.0	16.1	16.7
50 u	0.0653	--	0.0283	--	11.2	8.90

[a]Measured at 0.7 MHz.

TABLE VI

PROPERTIES OF ORIENTED HANDSHEETS

Sample No.	Basis Wt, g/m^2	Apparent Density, $\rho a, g/cm^3$	Shear Modulus, $\overline{G}_A$, GPa	Shear Strength, $\overline{\tau}_{max}$ MPa
100 r	98.1	0.788	0.110	2.32
100 u	117.9	0.834	0.313	5.28

In the torsion mode the failure is progressive from the circumference of the disk toward its center; i.e., the stress varies with radius. It was therefore of interest to determine if the samples had totally or only partially failed, since the majority of them had not separated into two halves.

Cross sections of the disks were examined using both light microscope and SEM techniques to confirm that the method of sectioning was not creating any artifacts. It was confirmed that the samples had indeed ruptured completely, i.e., A to B, as shown in Fig. 34 below:

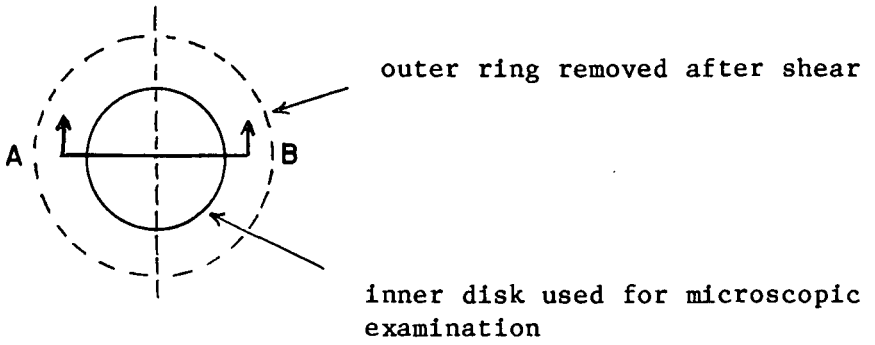

Figure 34. Specimen for light microscope and SEM examination.

Scanning electron micrographs of the cross sections are shown in Fig. 35a and 35b, and 36a, 36b, and 36c, for the restrained and unrestrained samples, respectively. It is interesting to note that for the sample dried without restraint there is a wavy fracture line, in contrast to the straighter line fracture of the restrained sample. In the case of the sample dried without restraint there appear to be fewer voids in the cross section. There are also more bridging fibers which serve to hold the samples together after failure. The freely dried (unrestrained) samples also tend to show more out-of-plane displacement, as might be expected from the wavy fracture line. Figures 36b and 36c taken at higher magnification clearly indicate interfiber bond failure. This is not so evident in the cross sections of the samples dried under restraint, Fig. 35b, although it is somewhat clearer in the in-plane views (see Fig. 37a and 37b).

In-plane views of the samples dried under restraint and freely dried are shown in Fig. 37a and 37b, and 38a and 38b, respectively. The differences between

the samples are not as evident as in the cross-sectional views. The in-plane views at 50X magnification suggest that failure may occur at islands or flocs, by delamination of that area. Furthermore, there does not appear to be any evidence of fiber failure.

The limited SEM evidence appears to be consistent with the mechanical testing results. The high shear modulus and strength of the freely dried samples could be from their denser cross section and the appearance of the fracture; i.e., the wavy fracture line indicates possibly that more area is involved in the fracture process.

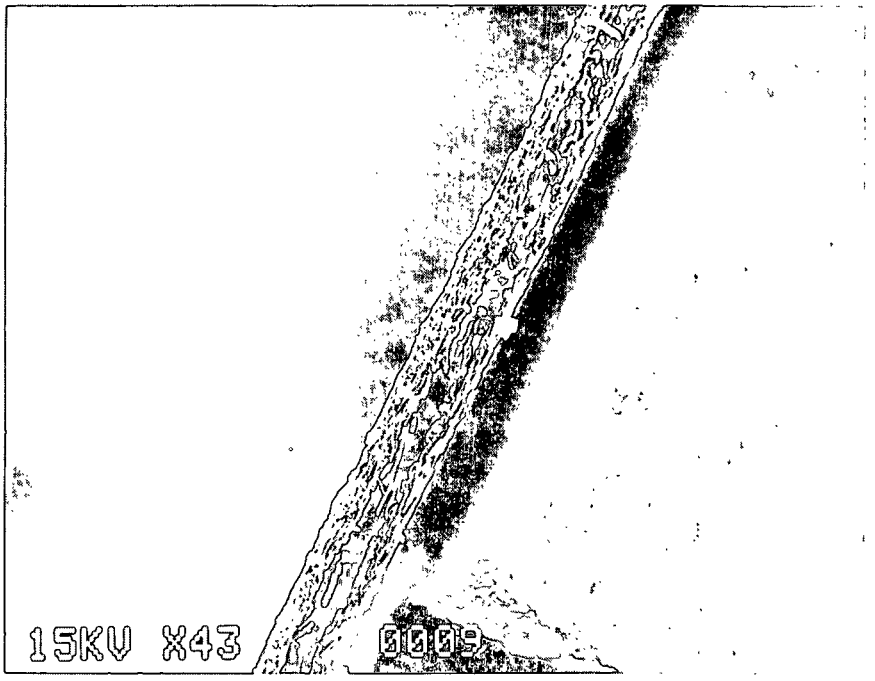

Figure 35a. Cross section of restrained sheet (sample 100 r at 43X).

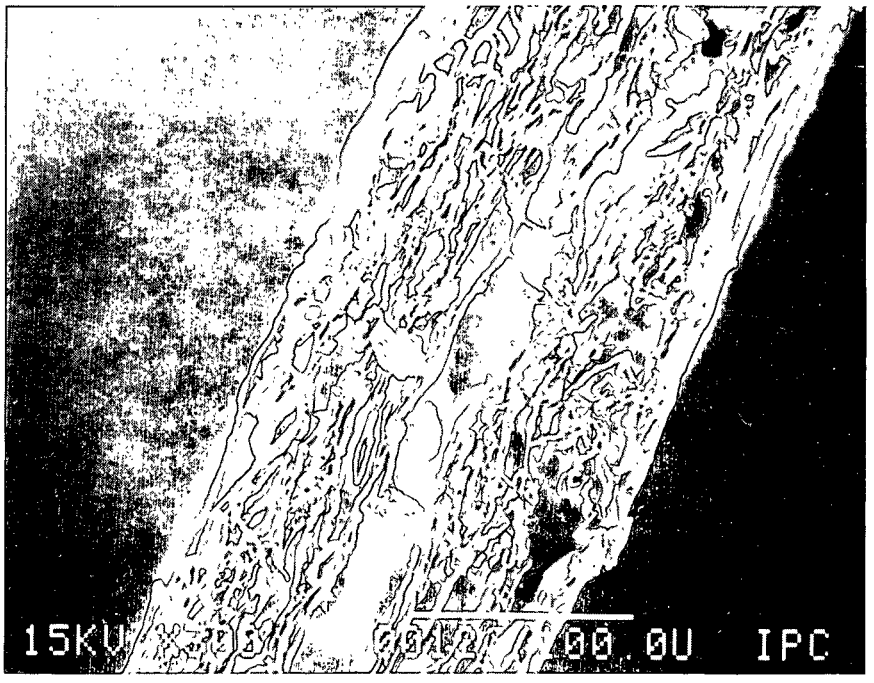

Figure 35b. Cross section of restrained sheet (sample 100 r at 300X).

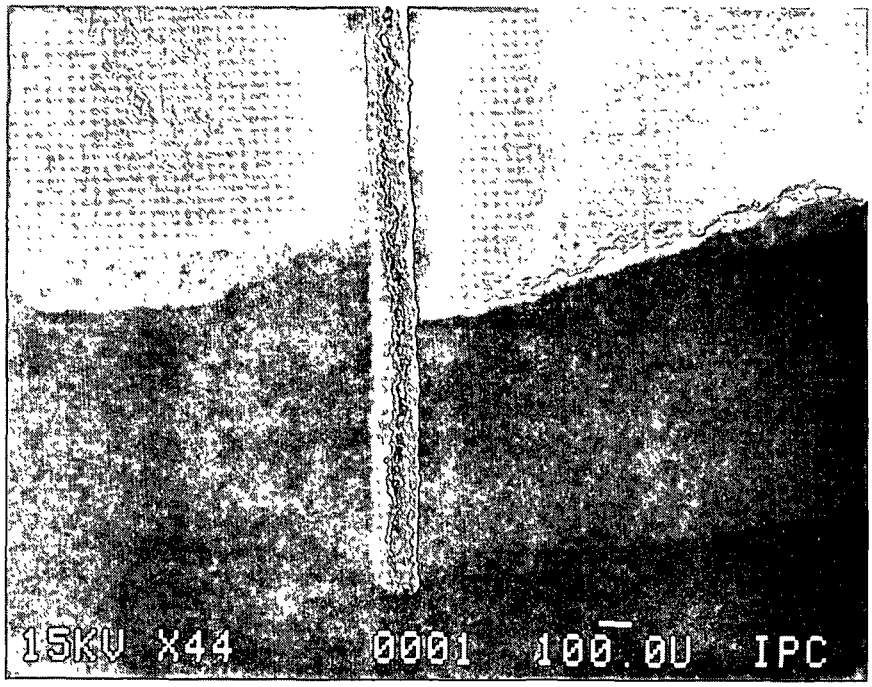

Figure 36a. Cross section of unrestrained sheet (sample 100 u at 44X).

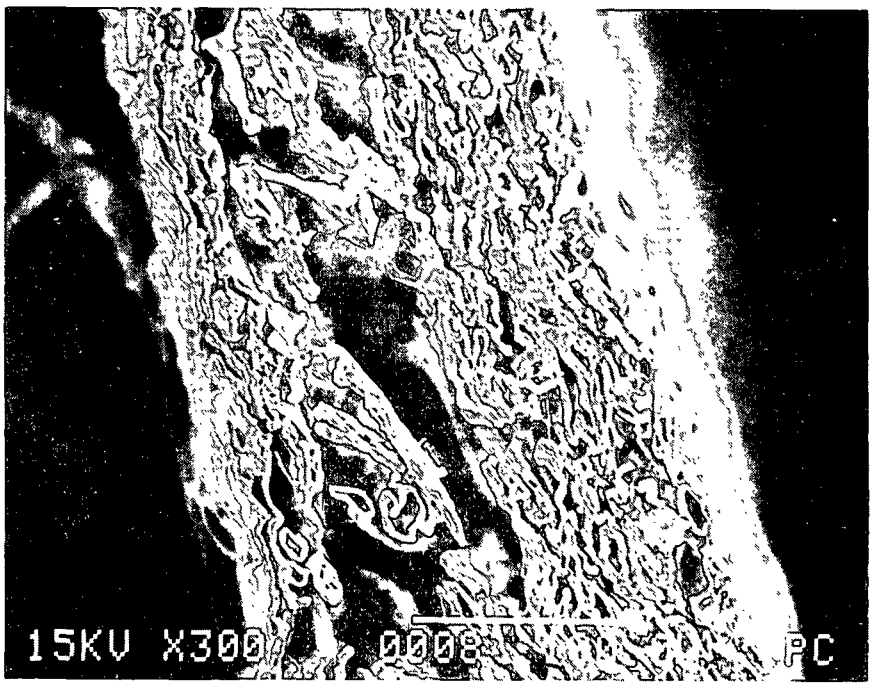

Figure 36b. Cross section of unrestrained sheet (sample 100 u at 300X).

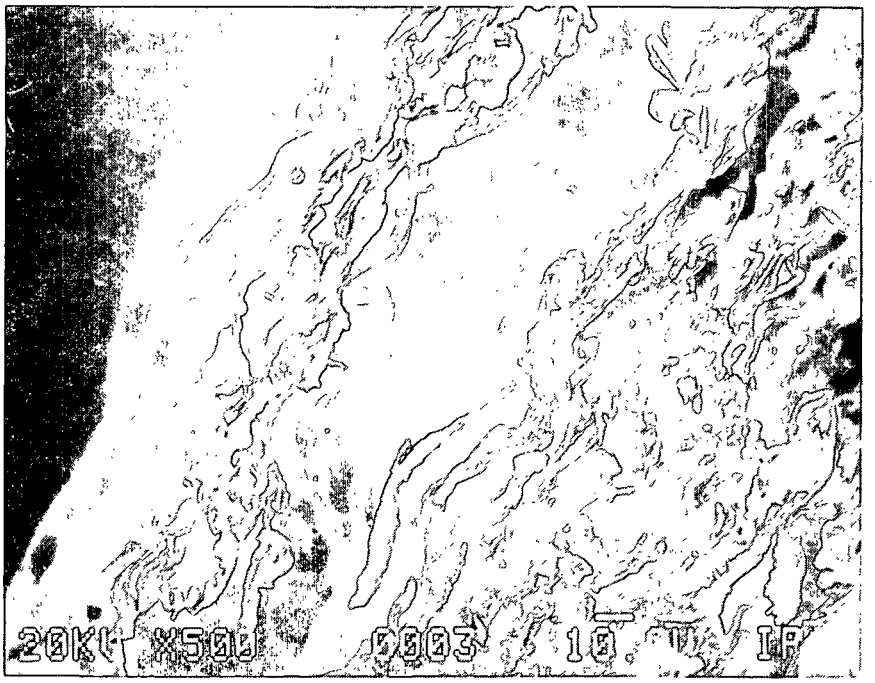

Figure 36c. Cross section of unrestrained sheet (sample 100 u at 500X).

Figure 37a. In-plane view of restrained sheet (sample 100 r at 50X).

Figure 37b. In-plane view of restrained sheet (sample 100 r at 300X).

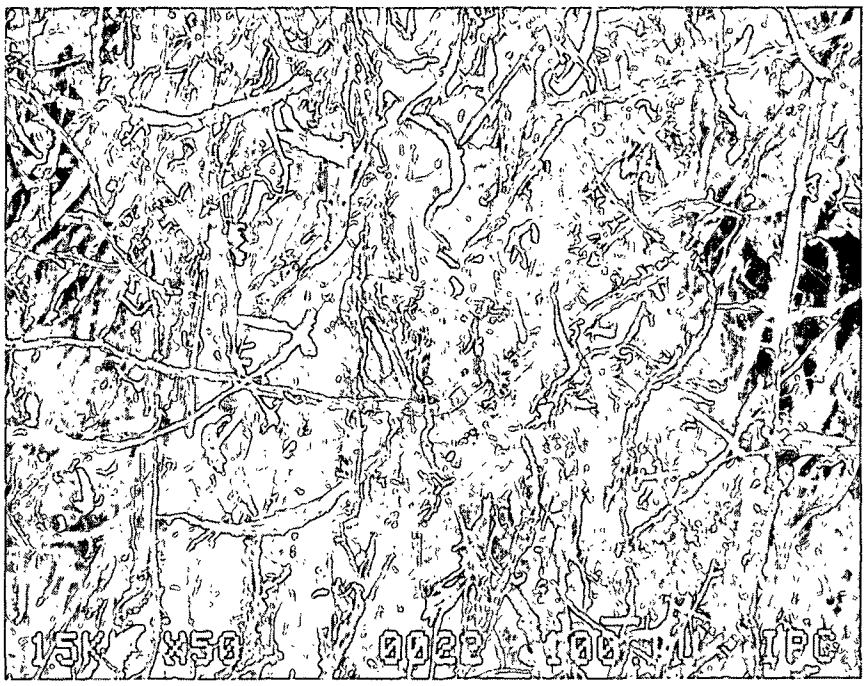

Figure 38a. In-plane view of unrestrained sheet (sample 100 u at 50X).

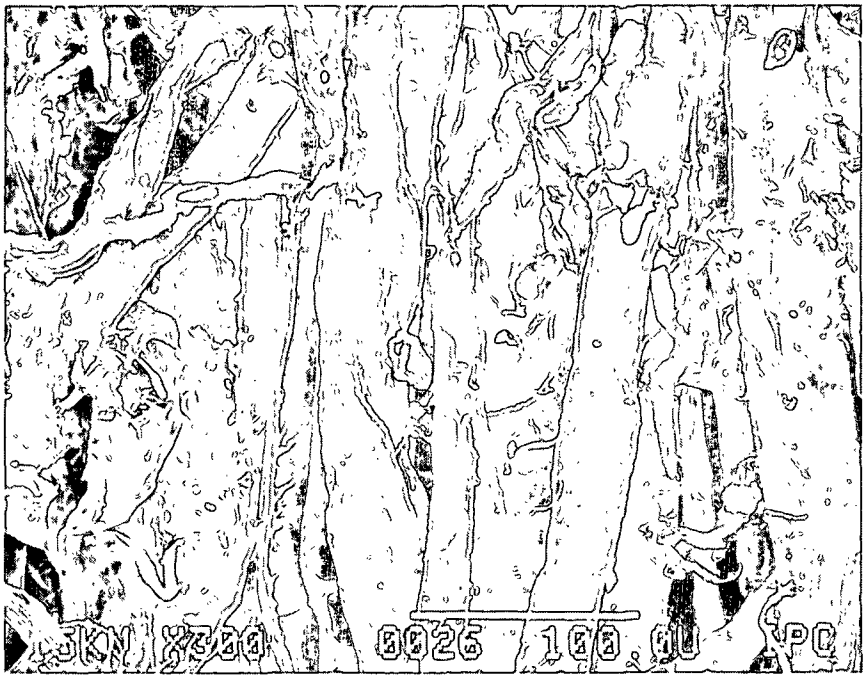

Figure 38b. In-plane view of unrestrained sheet (sample 100 u at 300X).

ACKNOWLEDGMENTS

The assistance of David Brennan and Betty John in performing the experimental work and of Sheila Burton in preparation of the manuscript is gratefully acknowledged.

LITERATURE CITED

1. Byrd, V. L., Setterholm, V. C., and Wichmann, J. F. Method for measuring the interlaminar shear properties of paper. Tappi 58(10):132-5(Oct., 1975).

2. Fellers, C. Procedure for measuring the interlaminar shear properties of paper. Svensk Papperstid. 3:(80)89-93(1977).

3. Heckers, W. and Gottsching, L. A method of testing in-plane shearing strength of paper and board. Papier 34:1-5(1980).

4. Perkins, R. W., Jr. and McEvoy, R. P., Jr. The mechanics of the edgewise compressive strength of paper. Tappi 64(2):99-102(Feb., 1981).

5. Perrizo, C. A291 Problem, July 1981.

6. Byrd V. L. Fiber orientation and drying restraint - effect on interlaminar shear and other paper properties. Svensk Papperstid. 15:105-9(Oct. 20, 1981).

7. Uesaka, T., Perkins, R. W., and Mark, R. E. Determination of Interlaminar Shear Modulus in Paperboard by the Torsion Pendulum Method. Private communication, T. Uesaka.

8. Wyk, W. V. and Gerischer, G. The influence of recycling on the strength properties of machine made paper. Paperi Puu 9:526-33(1982).

9. Whitsitt, W. J. and Sprague, C. Mechanics of fluting. Project 3396, Report One to Members of the IPC, June 15, 1983.

10. Goodier, J. N. An extension of St. Venant's Principle, with applications. J. Appl. Phys. 13, March 1942.

11. Setterholm, V. C. and Chilson, W. A. Drying restraint - its effect on the tensile properties of 15 different pulps. Tappi 48(6):634-40(Nov., 1965).

12. Setterholm, V. C. and Kuenzi, E. W. Fiber orientation and degree of restraint during drying. Tappi 53(10):1915-20(Oct., 1970).

13. Setterholm, V. C. A new concept in paper thickness measurement. Tappi 57(3): 164 (March, 1974).

14. Mann, R. W., Baum, G. A., and Habeger, C. C. Determination of all nine orthotropic elastic constants for machine-made paper. Tappi 63(2):163-6 (Feb., 1980).

15. Mann, R. W. Elastic wave propagation of paper. Doctoral Dissertation. Appleton, Wisconsin, The Institute of Paper Chemistry, Jan., 1979.

16. Fleischman, E. H., Jr. An investigation of the elastic and dielectric anisotropy of paper. Doctoral Dissertation. Appleton, Wisconsin, The Institute of Paper Chemistry, 1981.

17. Lekhnitskii, S. G. Theory of elasticity of an anisotropic elastic body. Holden-Day, Inc., 1963.

18. Wink, W., Personal Communication.

19. Htun, M. and DeRuvo, A. The influence of drying time and temperature on drying stress and related mechanical properties of paper. Doctoral Dissertation. STFI Stockholm, Sweden, 1981.

20. Cavlin, S. and Fellers, C. A new method for measuring the edgewise compression properties of paper. Svensk Papperstid. 9(78):329-32(1975).

21. Habeger, C. C. and Whitsitt, W. J. A mathematical model of compressive strength in paperboard. IPC Technical Paper Series, No. 130, Sept., 1982.

22. Wink, W. and Baum, G., A rubber platen caliper gage - a new concept in measuring paper thickness. IPC Technical Paper Series, No. 133, March, 1983.

23. Page, D. H. and Seth, R. Personal Communication.

THE INSTITUTE OF PAPER CHEMISTRY

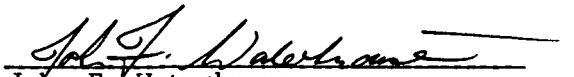

John F. Waterhouse
Research Associate
Paper Physics Section
Paper Materials Division

Gary A. Baum
Director
Paper Materials Division

APPENDIX

SHEAR MODULUS CALCULATION

CORRECTIONS FOR MOUNTING TISSUE AND ADHESIVE PENETRATION

The angular deformation measured includes the angular deformation of the mounting tissue. Furthermore, there is some degree of penetration of the mounting tissue adhesive into the surface layers of the board. In what follows we derive an equation to correct for these effects using the simple series model, as shown in Fig. 39 below:

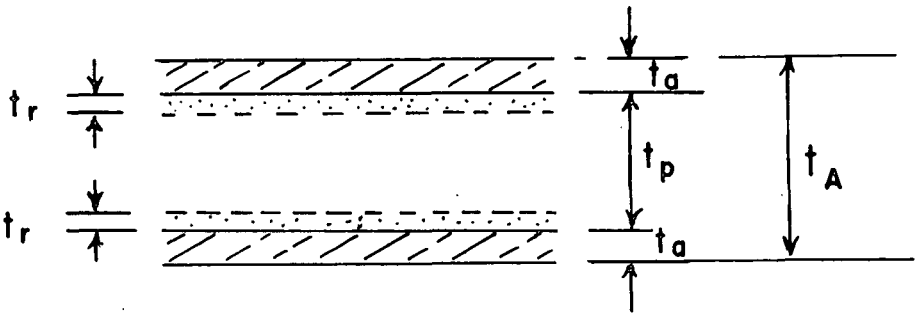

Figure 39. Sample and mounting tissue geometry.

In the figure, t_a, G_a, and ΔX_a are the thickness, shear modulus, and deformation of the mounting tissue layer, respectively; t_r, G_r and ΔX_r are the thickness, shear modulus, and deformation of the reinforced layer, respectively; and t_p is the paper thickness.

Assuming symmetry, the total deformation measured is:

$$\text{Total deformation} = 2\Delta X_a + 2\Delta X_r + \Delta X_p \qquad (1)$$

where ΔX_p is the deformation of the unreinforced paper "core," $t_p - 2t_r$.

An apparent modulus, G_A, can be defined as:

$$G_A = \tau / \left(\frac{\Delta X_p + 2\Delta X_r + 2\Delta X_a}{t_A} \right) \tag{2}$$

where τ is the applied shear stress.

Shear moduli for the mounting tissue, reinforced paper, and unreinforced "core" can be similarly defined:

$$G_a = \tau / \frac{\Delta X_a}{t_a}$$

$$G_r = \tau / \frac{\Delta X_r}{t_r} \tag{3}$$

$$G_p = \tau / \frac{\Delta X_p}{t_A - 2t_r - 2t_a}$$

In practice we calculate an apparent modulus G_A', which is defined as follows:

$$G_A' = \tau / \frac{\Delta X_p + 2\Delta X_r + 2\Delta X_a}{t_p} \tag{4}$$

Then from Eq. (2) and (4) we see that

$$\frac{G_A}{t_p} = \frac{G_A'}{t_A} \tag{5}$$

From the above equations we can, after some manipulation, solve for G_p in terms of G_A', the measured uncorrected shear modulus or apparent shear modulus. The result is:

$$1/G_p = \left(1 - 2(t_r/t_p)\right)^{-1} \cdot \left[\frac{1}{G_A'} - \frac{2t_r}{t_p} \frac{1}{G_r} - \frac{2t_a}{t_p} \frac{1}{G_a} \right] \tag{6}$$

Values of t_a and t_r can be estimated from caliper measurements on heat-activated tissues plus paper sample, and tissues only. Values of t_a and t_r are calculated as follows from caliper measurements on the paper sample alone, t_p, on two layers of mounting tissue after heat activation, $2(t_a+t_r)$, and on the heat-activated mounting tissues and paper sample, (t_p+2t_a), then:

$$2t_a = (t_p+2t_a) - t_p. \tag{7}$$

$$2t_r = 2(t_a+t_r) - 2t_a. \tag{8}$$

Mounting Tissue Shear Modulus, G_a

Using the procedures given in the Experimental Section, the shear moduli of multiple layers (2 to 10 layers) of mounting tissue were measured. The shear modulus values showed considerable variability, but it was also found that there was a significant variation in the apparent density of the mounting tissue after mounting and heat activation. The variation of mounting tissue shear modulus with apparent density is shown in Fig. 40.

Using Eq. (6) above, and assuming $G_a = G_r = 0.550$ GPa, corrected values of shear moduli for surface ground corrugating medium and linerboard samples are shown in Tables VII and VIII.

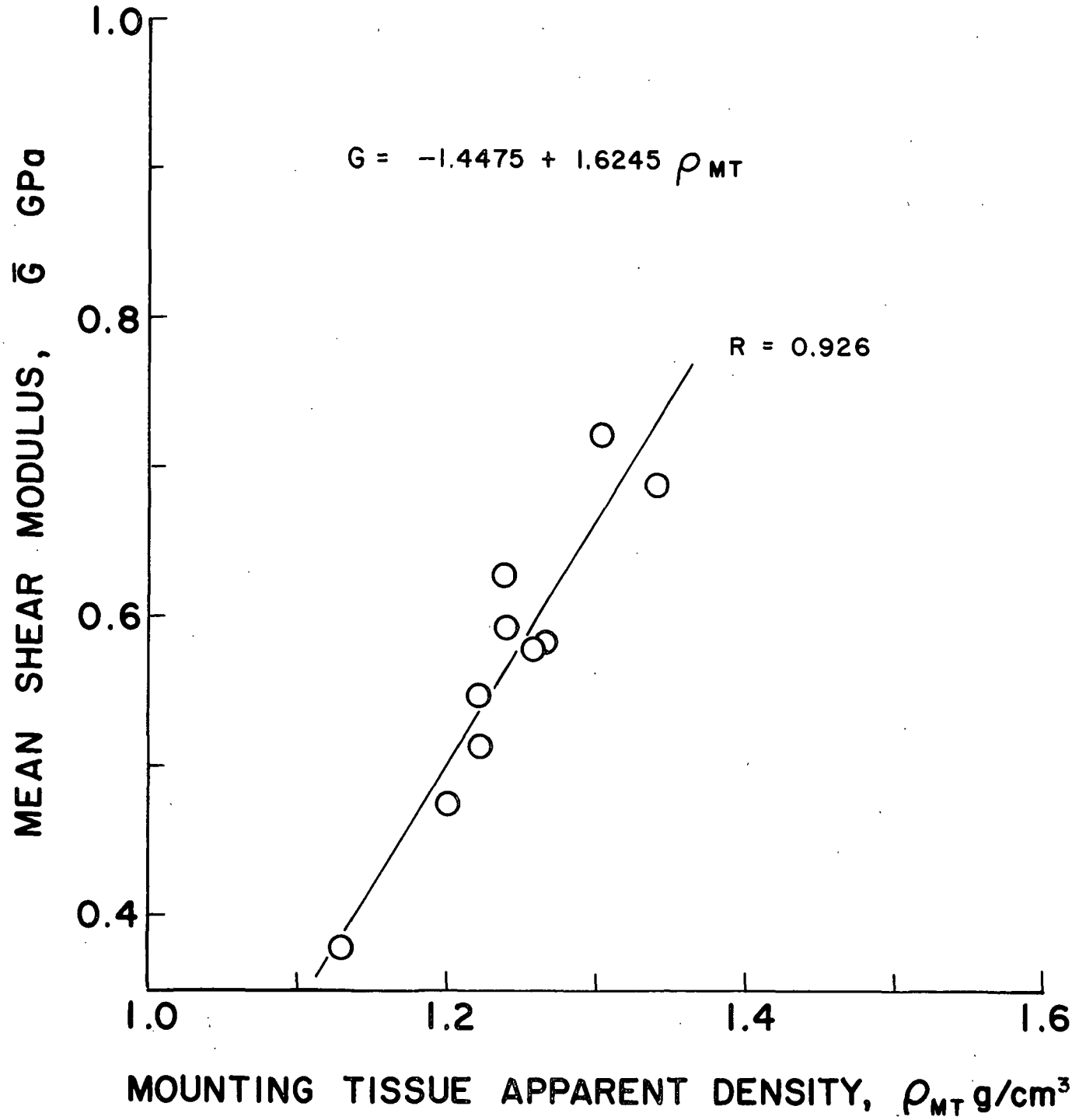

Figure 40. Effect of mounting tissue density on mechanical shear modulus.

TABLE VII

SURFACE GROUND CORRUGATING MEDIUM

#	BW g/m^2	$2(t_a+t_r)$, in	$2t_a$, in	$2t_r$, in	t_p, in	G_A', GPa	G_p, GPa	ρ, g/cm^3
1	134.5	0.0044	0.0016	0.0028	0.0108	0.157	0.131	0.491
2	131.4	0.0044	0.0025	0.0019	0.0083	0.192	0.181	0.624
5	109.8	0.0044	0.0023	0.0021	0.0062	0.237	0.225	0.698
7	75.9	0.0044	0.0025	0.0019	0.0042	0.306	0.399	0.712

TABLE VIII

SURFACE GROUND LINERBOARD

#	BW g/m^2	$2(t_a+t_r)$, in	$2t_a$, in	$2t_r$, in	t_p, in	G_A', GPa	G_p, GPa	ρ, g/cm^3
1	213.7	0.0044	0.0022	0.0022	0.0125	0.0914	0.0800	0.674
3	183.8	0.0044	0.0022	0.0022	0.0107	0.0779	0.0657	0.677
5	136.9	0.0044	0.0023	0.0021	0.0083	0.0839	0.0682	0.650
7	105.2	0.0044	0.0024	0.0020	0.0065	0.0988	0.0778	0.638
9	68.1	0.0044	0.0024	0.0020	0.0041	0.1757	0.1370	0.654